ADDIS ABABA UNIVERSITY
ADDIS ABABA INSTITUTE OF TECHNOLOGY
SCHOOL OF CIVIL AND ENVIRONMENTAL ENGINEERING

ACCURACY ASSESSMENT OF DIGITAL SURFACE MODEL FROM AERIAL IMAGES: CASE STUDY OF NIFAS SILK SUB CITY, ADDIS ABABA

Thesis Submitted to the School of Civil and Environmental Engineering, in Partial Fulfillment of the Requirements for the Degree of Master of Science in Geodesy and Geomatics (Specialized in Geomatics)

Prepared by: Jemal Endrie Ali
(ID No: GSR/2586/16)

Advisor: Andenet Ashagrie (Dr.)

March, 2022
Addis Ababa Ethiopia

ADDIS ABABA UNIVERSITY
ADDIS ABABA INSTITUTE OF TECHNOLOGY
SCHOOL OF CIVIL AND ENVIRONMENTAL ENGINEERING

ACCURACY ASSESSMENT OF DIGITAL SURFACE MODEL FROM AERIAL IMAGES: CASE STUDY OF NIFAS SILK SUB CITY, ADDIS ABABA

By: Jemal Endrie Ali

(ID No: GSR/2586/16)

Advisor: Andenet Ashagrie (Dr.)

March, 2022
Addis Ababa Ethiopia

Declaration

I declare that this thesis is a result of my own research observations and findings. Sources of information other than my own have been acknowledged and a reference list has been appended. This work has not been previously submitted to any other University for award of any type of academic degree.

Name of the student	Date	Signature
_____	_____	_____

Name of advisor	Date	Signature
_____	_____	_____

ADDIS ABABA UNIVERSITY

ADDIS ABABA INSTITUTE OF TECHNOLOGY

SCHOOL OF CIVIL AND ENVIROMENTAL ENGINEERING

This is to certify that the thesis prepared by Jemal Endrie Ali entitled: Accuracy Assessment of Digital Surface Model derived from Aerial Photograph Images: The Case of Nifas Slik Sub-city, Addis Ababa submitted in partial fulfillment of the requirements for the Degree of Masters of Science (in Geodesy and Geomatics Specialize in Geomatics) complies with the regulations of the university and meets the accepted standards with respect to originality and quality.

Andent Ashagrie (Dr.)	_____	_____
Advisor	Signature	Date
_____	_____	_____
Internal examiner	Signature	Date
_____	_____	_____
External examiner	Signature	Date
_____	_____	_____
External examiner	Signature	Date

Acknowledgements

First and for most I would like to give my heartfelt thanks to the almightily ‘ALLAH’, who paved all the ways through which I have travelled to reach at this position. Next, I like to express my deepest gratitude to my advisor Andenet Ashagrie (Dr.) for his constructive advices and suggestions while I was writing this thesis. He gave me constructive comments and critical reviews that make this study a success. His support and advice makes me motivated and energetic all the way through this study.

I would like to express my gratitude to my office staffs of Nifas Silk landholding adjudication project office specially, Berket Belay, Eliyas Tukye, Melkamu Tarekegni and Getasew Tilahun for permitting me to pursue this study. I also would like to thanks Addis Ababa University and the ministry of urban development and housing for granting the financial support for this research.

I wish to the special thank for all organizations and individuals of INSA and EMA that contributed in my study by providing me data for this research.

I would also like to thank all my family members who helped me in different ways to make the writing of this thesis possible. I am particularly indebted to my mother Zenebeh Dawode and my father Endrie Ali without whom I would not be at this position; finally I would like to thank my friends and those who helped me in any way while I was writing this paper.

Abstract

Airborne aerial photograph is one of the most effective means of terrain data collection. The vertical accuracy of DSM derived from 2010 and 2016 collected aerial photograph in urban area of Nifas Silk sub city is the critical point in this research. In this study, the reference level produced from GPS elevation, existed GCP elevation and differential leveling are measured to assessed the vertical accuracy of existed GCP elevation and both DSM elevation data derived from Airborne aerial photograph for building urban land cover types. Using static GPS elevation as a reference, the accuracy of existed GCP elevation gave a RMSE value of ±1.049m and an arithmetic mean value of 1.049m. GPS reference elevations gave us the RMSE value of ±0.592m and ±0.787m and an Arithmetic Mean value of ±0.466 and ±0.659 for used DSM derived from 2010 and 2016 aerial photograph respectively. On the other hand, by using GCP as reference elevation, gave the RMSE value of ±0.415m and ±0.486m and also used differential leveling elevation, gave the RMSE value of ±0.68m and ±0.911m for used both DSM derived from2010 and 2016 aerial photograph respectively. A spatial analysis tools can be used for the extraction of DSM elevation in arc GIS software package. Finally, 1.96xRMSE and frequency histogram statistical measurements of data analysis are performed for the difference between measured independent checkpoints and corresponding point of both DSM derived from the two aerial photographs. For our study area, using the three reference elevation point of existing GCP, RTK GPS and Leveling measurements, DSM derived from (2010) aerial photograph elevation data have an accurate by A RMSE value of ±0.071m, ±0.198m and ±0.231m and/or Absolute Mean value of ±0.071m, ±0.198m and ±0.379m that of the value of DSM derived from (2016) aerial photograph data respectively.

Keywords: Ground Control Point, Remote Sensing, Global Positioning System, Photogrammetry

Table of Contents

Contents **Page**

List of Tables

Page

List of Figures

Page

List of Abbreviations

3D	Three Dimensional
AACA	Addis Ababa City Administration
ASPRS	American Society for Photogrammetry and Remote Sensing
CCD	Charge-Coupled Device
DEM	Digital Elevation Model
DSM	Digital Surface Model
DTM	Digital Terrain Model
EGM	Earth Gravitational Model
EMR	Electro Magnetic Spectrum
FIR	Far Infrared
GII	Geospatial Information Institute
GS	Geodetic System
GNSS	Global Navigational Satellite System
GPS	Global Positional System
GCP	Ground Control Point
GDEM	Gridded Digital Elevation Model
GSD	Ground Sample Distance
IMS	Inertial Measurement System
IMU	Inertial Measurement Unit
INS	Inertial Navigation System
INSA	Information Network Security Agency
IFOV	Instantaneous Field of View
ICSM	Inter-Governmental Committee on Surveying and Mapping
IGS	International Geodetic System
LGO	Leica Geo-office
LiDAR	Light Detecting and Ranging
MSL	Mean Sea Level
MIR	Mid Infrared
MSS	Multispectral Scanner
NIR	Near Infrared
RADAR	Radioactive Detecting and Ranging
RTK	Real Time Kinematic
RS	Remote Sensing
RMSE	Root Mean Squire Error
SRTM	Shuttle Radar Topography Mission
TIN	Triangular Irregular Network
UV	Ultra Violet
UTM	Universal Transverse Mercator
WGS	World E Geodetic System

CHAPTER ONE

1. Introduction

1.1 Background

"A Digital Elevation Model (DEM) is a three dimensional representation of the bare ground surface without any object, like plant and buildings". There is some confusion in the use of the terms DEM, DSM and DTM. We are going to consider the term that Digital Surface Model (DSM) on the other hand represents the surface of the earth and includes all objects on it. All captured data from satellite are originally DSM (Maune et al., 2007, p.32) and (ASPRS, 2004). The term DTM would be a model in which the elevations are referred to the bare ground. DEM are often used in geographic information system and were the most common basis for digitally produced relief maps which was called topography map. Topography maps exist in digital or analog form and represented by contour line, gridded and TIN structure to show the elevation of the surface in the area. We are going to deal with the second of grid format as it is currently the most widely used for DSMs treatment. Grid models are conformed as a regular-rectangular array of cells each of which stores an attribute value, so the area of each cell adopts the same elevation value, producing a sudden change in the limits of each cell, the elevation is represented by the cell of the grid. Thus, the size of the cell, or resolution, is a key parameter. This parameter is related to the traditional concept of scale and great spatial detail. Large cell sizes, giving small resolution, are linked to small scale and less spatial accuracy. Therefore, there is a direct relationship between resolution and accuracy: the higher resolution, the greater expected accuracy, and *vice versa*.

There are three basic data sources for the creation of DSM relying on ground-based, airborne and space-borne surveying techniques. These techniques can be compared considering four aspects (i.e., price, accuracy, sampling density, preprocessing requirements). Each technique has its particular advantages but also some disadvantages. Nowadays, surveying engineers frequently use aerial photograph and remote sensing rather than direct survey data to get the position of spatial phenomena. The importance of airborne and space born observation are evident: air craft and satellite carrying a variety of camera and sensor and looking toward the earth can collect data, at relatively low costs, broadly consistent with the required spatial, spectral and temporal

resolutions to interpolate new DSMs. According to Kennie and Petrie stated that in reporting (Hirt, 2015) traditional ground-based methods are very accurate, but tedious, and therefore mostly limited to small areas. Field surveying based on tachymetry delivers terrain heights at selected locations. But, Satellite based surveying techniques (GNSS) provided terrain heights at discrete locations, or along profiles (e.g., roads). Another source of terrain heights are digitized contour lines from existing topographic maps (spot heights). Unlike, ground surveying; modern airborne- and space-borne sensors are considerably more efficient for terrain surface mapping than ground methods. This was because the terrain is sampled at a vast number of locations in little time, and the sensor movement in air or space allows mapping of regional or even global profiles. Important mapping sensors on flying platforms are (i) image-based (photogrammetry), (ii) laser-based (lidar), and (iii) radar-based (e.g., radar interferometry). Aerial photogrammetry method is an issued that used to produce digital surface model generation. It also an accurate and powerful tool in surface model generation, producing high resolution of DSM by means of triangulation (Fabris and Pesci, 2005), very high-resolution aerial imagery are currently available for modeling more detailed earth surface process (Jarvis et al. 2004, p.32)**.** On the other hand, Photogrammetric methods (e.g., Baltsavias 1999, p.11) use overlapping pairs of images showing the terrain from different angles (stereo principle). Stereoscopic processing yields terrain heights for ground points captured and identified in both images.

Measurements were made to determine unknown quantities. All measurements contain error. These types' of errors were happened when measurement is performed and the method and technical data processing to be achieved. DSM data derived from aerial photograph was vulnerable by those types of errors. For example, aerial photograph is influenced by different factors that have been investigated separately, such as the camera's focal length, the flight altitude and camera orientation, landscape variation, earth's curvature, scale of photograph, technical procedures like, rectification and image exposure as well as the image quality (Michael et al., 2016, Pp.41). Additionally, quality, the number and spatial distribution of Ground Control Points (GCPs) used for georeferencing the acquired images have been cited as one of the most important factors affecting image qualities (Kaab et al., 2014). For instance, check point's data were brought from independent sources and be at least three times more accurate than the data set to be tested (NDEP, 2004). Several studies investigated the effect of varying number, quality

and position of GCPs on DSM accuracy, (Shahbazi et al., 2015) for instance, did several tests varying the number and locations of GCPs, as well as the number of images where the GCPs are visible. They found that the image georeferenced with a larger number of GCP are more accurate than an image georeferenced with few and that an evenly distributed GCP-network generates high accuracy of DSM data than a network in which GCPs are clustered. They also showed that DSM accuracy is higher when the GCPs are installed in a way that they are visible on many images. The studies of (Tahar et al., 2012), (Tahar, 2013), as well as (Rosnell and Honkavaara, 2012) also concluded that DSM accuracy increases with increasing number of GCPs. A similar conclusion was made in the study of (Tonkin and Midgley, 2016), who additionally showed that when a certain number of GCPs is reached, the DSM accuracy does not increase further. All of these studies, however, performed their accuracy assessments on flat or undulated terrain and on well-structured surfaces, which facilitate DSM construction.

In Ethiopia, the City Government of Addis Ababa Integrated Land Management Information System Project Coordination (AACA) and Geospatial Information Institute (GII) established well distributed and visible each other of ground control points in Addis Ababa city in July 2011. This survey marks was produced high quality of horizontal and vertical position based on the reference system of UTM Zone 37N Projection System, Clark 1880 (ellipsoid), Adindan Reference Datum and EGM96 Height reference (Gizachew, 2012, p.2).

On the other hand; the accuracy of DSM derived from aerial photograph was affects by the type of ground cover because, the building and vegetation can limit ground detection. Areas with building and vegetation tend to cause greater elevation errors than open terrain does (NDEP, 2004).This study is only restricted in urban area (Nifas Silk Sub city). Therefore, the check points should be distributed over the building cover type features in the study area.

At a national level, DSMs existed for many countries at varying resolution, different data acquisition method: ground-based, airborne lidar and photogrammetric surveys. Those data derived from different method have a fundamental role in geosciences and engineering, and have numerous applications. Publically available DSM with continental and local coverage originate from airborne topographic mapping missions were conducted for a purpose of cadastral and topographic mapping and extensive set of disciplines such as civil engineering hydrology, geomorphology, and prevention of the natural disasters like floods, fires etc. in a recent time,

Ethiopia developed high resolution aerial images and accurate land information. The government was made a system development orthophoto generation and cadastral information for 23 towns including the capital city of the country. In Addis Ababa, Hansa Luftbild proposed a technical flight mission in the time of 2010 with a scale of 1:2000 and at ground sample distance (GSD) of 0.2cm with a vertical resolution of 10m to updated the existed data and covers the whole area of the city. Six years later, for rural cadastral information, photogrammetric surveying was conducted by Information Network Security Agency (INSA) in 2016 with an estimated scale of 1:48048 and at ground sample distance (GSD) of 0.25cm with a vertical resolution of 10mx10m. Finally, the data acquired by aerial photograph method were a fundamental requirement for elevation accuracy assessment in the study area.

1.2 Statement of the Problem

Nowadays, the Digital Surface Model (DSM), which is a 3D digital representation of an elevation surface over a specific area, is one of the sciences most fundamental requirements for a large variety of spatial analysis and modeling problems in environmental. It is used in the analysis of ecology, hydrology, agriculture, geology, geomorphology, and urban planning modeling for the infrastructure activities, as a means of both explaining process and predicting them through modeling (Schumann et al., 2008). On the other hand, DSM data is a necessary input parameter for determining the extent of watershed and drainage network, determining the slop and aspect associated with a geospatial modeling and planning for telecommunication, image rectification, preparing 3D reproduction, 3D perspectives and flight simulations**,** agricultural applications studies of landscape dynamics and land form characterization of volcanoes (Maune et al., 2007**)**.

Exact information about the earth surface is the fundamental importance in all its applications area. The topography exaggerates control over range of earth surface processes (evaporation, water flow, mass movement, forest fires) important for the energy exchange between the physical climate system in the atmosphere and bio-geochemical cycles at the earth surface. Due to this application of DSM in the study area, users and the government investigates the dependences of all life forms and their environment, needs the knowledge about the relief to model the movement of water, describe the relief recognizing form building process and investigate the variability of temperature moisture, air particles influenced by topography.

Currently, assessing the vertical elevation derived from aerial photograph is critical because there are a lot of problem and function in many applications. Inadequate and inaccurate elevation data can lead to poor decision that will have a negative impact in our environment and the associated human, cultural and physical landscape. Still a limited number of studies have addressed the issue of accuracy assessment of DSM derived from aerial photograph. In the previous studies reported, the vertical accuracy of DSM derived from aerial photograph was 0.55m with a photo scale of 1:9000 and flight altitude of 5000m above the terrain surfaces (Giuseppe P., and Francesco F. 2013). On the other study reported, the statistical test for DSM and DTM demonstrates that the mean elevation error respectively yields around 0.41m and 0.48m the RMSE about 0.48m and 0.47 with a 1:5000 scale (Lella, et al., 2012). And also the choice of an elevation data is a matter of preference and it may be related to cost of data production. With respect to the geometrically simpler shape of a perfect ellipsoid, the Earth's topographic surface is irregular and complex. The task of mapping a level surface on the surface of the earth is challenging. Due to a development of GNSS, Now a day we can obtain accurate elevation data of the terrain distribution without necessarily carrying out the tedious and time-consuming procedures of geometric or trigonometric leveling (Hirt, et al., 2011, Gruber et al., 2011). Although, the elevation data obtained from aerial photograph is originally called ellipsoidal heights. This elevation was not applicable in large scale DSM derived from aerial photograph. So, there is a need for a new approach which computes height of the desired filed point by referring to the national standard parameter adopted by EGII.

There are many methods of assessing elevation accuracy that can be applied to DSMs. These methods have evolved from the NMAS (National Map Accuracy Standard) to the most recent, complex and sophisticated: the ASPRS Positional Accuracy Standards for Digital Geospatial Data. In the study area, the national standard adopted by EGII, the accuracy of the data derived from aerial photograph was not exceeds three times of the pixel size of ground distance in elevation. The purpose of this paper is to investigate the quality of DSM derived from both aerial photographs when collected in the year of 2010 and 2016 in Nifas Silk sub city.

1.3 Objectives

1.3.1 General objective

The main objective of this study was to assess and evaluate the vertical elevation data of DSM derived from both aerial photograph using selected checkpoints in the study area.

1.3.2 Specific objectives

The specific objectives of this study were:

- To evaluate the accuracy of the existing ground control points in the study area
- To assessing the elevation point of DSM data which derived from 2010 aerial imageries.
- To assessing the elevation point of DSM data which derived from 2016 aerial imageries.

1.4 Significance of the Study

This research entitled as assessing the vertical accuracy of DSM which derived from aerial photograph provide information to application users in the field of commercial and public business and management fields, navigation, flow of energy, risk management, planning and construction fields, land cover classification fields, governmental decision making and many more.

On the other hand, it also provides exact information about the earth's topography in all geosciences to model for a variety of application in the study area. It also provides information about the effective and usefulness of both data to the stakeholders for spatial modeling purpose.

1.5. Scope of the Study

This research focuses on the positional accuracy specially the evaluation of vertical accuracies of DSM data which was collected in 2010 and 2016. It covers all Nifas Silk sub city of Addis Ababa city administration area. A complete assessment of vertical elevation of both DSM data and five static GCP points have required too much time and material like GPS receiver and rod leveling for the measurement of 24 and 10 sample checkpoints in the area of Nifas Silk sub city in a major land cover area of building respectively.

1.6 Limitations of the Study

For comparing the elevation difference between both DSM data with GCP points and the checkpoints in the project area a lot of issues and difficulties occurred in the process. Due to the already developed high resolution aerial images and accurate land information; government offices were not willing to provide these data. Because the data have been prepared and processed for urban security and geospatial modeling. So, we have got a difficult to gather these existed data from the Ethiopian Information Network and Security Agency (INSA) and EGII. And also, it is difficult to get complete information that is used for accuracy assessments in the responsible government office. On the other hand, instrument like GPS receiver and leveling, materials and licensed software for data processing and analyzing purpose were not presented or/and difficult to purchase the data that existed in the government office. Observing the checkpoint elevation data there have been some limitation encountered by the researcher. The first one was Absence or damaged of the existed GCP points that randomly selected from total GCP points. And the other one was systematic and gross errors have been occurred in the time of measurements; that was personal, bad environmental condition or instrumental.

1.7 Organization of the thesis

This paper is organized in to five chapters. The first chapter that is chapter one contains an introductory part of the paper. Chapter two deals with the related literature review of the study. Chapter three includes descriptions of study area, the data and the methodology for conducting the research. Chapter four focuses on the major findings of the results and analysis of the collected data. The last chapter, chapter five draws conclusion and proposes some possible recommendations.

CHAPTER TWO

2. Literature Review

2.1 Height systems

To determine heights of earth points, an origin surface with zero height must be described and the vertical distance of points from the surface must be determined. For heights, a variety of surfaces can be taken as reference. Of these, the most important surface is the geoid. Reference surfaces and vertical distances of points from the surfaces have different physical and geometric meanings. Geodetic heights also have different physical and geometric meanings. Thus, scholars introduce several height systems amongst all some basic height systems were examined as follows.

2.1.1 Orthometric height

Orthometric height is the height of a point above the geoid (equipotential surface of the Earth or above mean sea level), and the orthometric height (H) difference would be the difference between the ellipsoidal heights (h) and the normal height (N) of two points. Orthometric heights are the distance of a surface point along the plumb line to the geoid, which is taken as the reference surface, is named the orthometric height (H). It is also a natural "heights above sea level", that is, heights above the geoid. Therefore, they have an unequalled geometrical and physical significance. It was the best height system in geodetic science. It can be obtained as follows:

$$\boldsymbol{H = h - N} \qquad \mathbf{2}.1$$

From the above relationship the ellipsoid height (h) was the height of a point above the surface of ellipsoid. Ellipsoid height was easily calculated from Cartesian EFEC coordinates. The Geoid height of (N) was the height above or below the ellipsoid calculated.

2.1.2 Normal height

Normal height system consists of quasigeoid as a datum and "Normal heights", H, measured along normal gravity plumb line. Gravity values are needed to convert observed height differences into normal height differences. How is a (practical) height system realized in practice? There are two issues here: realization of the datum, i.e., the "practical datum" and

transformation of observed (leveled) heights to “proper heights” (in a transformation that makes use of real gravity values). Normal heights are referenced to a datum called quasigeoid, a computed artificial surface introduced by Molodenskij that runs within two meters on each side of the geoid. The quasigeoid also needs to be referred to the reference ellipsoid. Practical datum for normal is the same as for orthometric heights. Normal heights are not physically meaningful but would be geometrically interpretable if it were not for the quasigeoid. Both orthometric and normal heights may be derived from potential numbers or dynamic heights, both the latter being physically meaningful.

2.1.3 Geodetic height

Geodetic heights were never meant to serve as practical heights. They are not observable by terrestrial techniques. Their datum is the reference ellipsoid, hypothetical surface, adopted by convention. Geodetic heights h are computed from 3D satellite determined positions as accurately as implied by the accuracy of the 3D positions. They are measured along the normal to the ellipsoid and are sometimes incorrectly called “ellipsoidal heights”. No gravity is needed in their determination. But they are very important in measuring congruence of other height systems. The concept behind geodetic height determined from Cartesian geocentric position of x, y, z from GNSS satellites observation. It gets transformed into the geodetic curvilinear coordinate system referred to a geocentric reference ellipsoid of revolution of major semi-axis (a) and eccentricity (e). due to a wide scale of geometric reference the height of the data was not applicable in local vertical determination.

2.1.4 Earth Gravitational model

Accurate knowledge of the gravitational potential of the Earth, on a global scale and at very high resolution, is a fundamental prerequisite for various geodetic, geophysical and oceanographic investigations and applications. Over the past 50 or so years, continuing improvements and refinements to the basic gravitational modeling theory have been paralleled by the availability of more accurate and complete data and by dramatic improvements in the computational resources available for numerical modeling studies. These advances have brought the state-of-the-art from the early spherical harmonic models of degree 8 [Zhongolovich, 1952], to the present solution that extends to degree 2190. Rapp [1998] provided a brief review of the major developments in global gravitational field modeling over the 20th century. The best known global geoid model is

the National Geospatial -Intelligence Agency/National Aeronautical and Space Administration (NGA/NASA) WGS 84 EGM96 Geopotential Model, hereafter refer to as EGM96. This product is a set of coefficients complete to degree and order 360, a companion set of correction coefficients needed to compute geoid height over land and a geoid height grid posted at 15 arc-minute spacing. The other one is Earth Gravitational Model (EGM 2008) to degree 2160 is progressing with the availability of improved versions of a complete and accurate 5′×5′ worldwide global gravity anomaly database and GRACE-derived satellite solutions that takes advantage of all the latest data and modeling for both land and marine areas worldwide. The development of the final model, designated EGM2008, was completed in late March 2008, and EGM2008 was presented and released to the scientific community on April 17, 2008 [Pavlis et al., 2008]. Finally, the model was used for calculating of the normal undulation of the elevation of the Geoid below or above the ellipsoidal height of the point.

From the above height system, we conclude the best system to use as reference datum. The datum, Geoid, is very smooth surface, convex everywhere at sea as well as the land that is an ideal for a datum. The datum approximates the average mean sea level and this satisfies the usual practical requirements. orthometric height have a clear geometrical interpretation and dynamic height have a clear physical interpretation. Because the classical system is congruent, orthometric height can be also determining simply as difference of geodetic and geoidal height.

2.2. The concept of DEM, DSM and DTM

The earth surface is a continuous phenomenon. There are various ways of representing such terrain surface in digital form using a finite amount of storage. These forms of elevation are: Digital elevation model (DEM) is the digital elevation of the land surface elevation with respect to any reference datum. DEMs are used to determine terrain attributes such as elevation at a point, slope, and aspect (orientation). Digital elevation models (DEMs) play an important role in terrain-related applications. Researches on terrain data collection and DEM generation have received great attention. Traditional methods such as field surveying and photogrammetry can yield high-accuracy terrain data, but they are time consuming and labour-intensive (Theobald, 1989). DEM were used to be developed from the contours mapped in the topographic maps or stereoscopic area images. From this point of view, Digital Elevation Model (DEM) is defined as “any digital representations of the continuous variation of relief cover space” (Borough and

McDonnell, 1998**),** where relief refers to the height of earth surface with respect to the datum considered. It can also be considered as regularly spaced grids of the elevation information, used for a continuous spatial representation of any terrain.

Many researcher Digital terrain model (DTM) and Digital surface model (DSM) are often used as synonyms of the DEM. Technically a DEM contains only the elevation information of the surface free of vegetation, building and often non-ground objects with reference to a datum, such as Mean Sea Level (MSL). The DSM differs from DEM as it includes the top of building, power line, tree, and all objects as seen in synoptic view. On the other hand, in a DTM, in addition to the elevation information, several other information are included, viz, slope, aspect, curvature and skeleton. It thus gives continuous representation the smoothed surface.

DEM or DSM generated by using the elevation information from several points, spaced at regular or irregular interval. The elevation information may be obtained from different sources like field survey, topographic contours, etc. DEM uses different structures to acquire or store the elevation information from various sources. In order to fully represent the terrain surface, a model has to be established to define the relationships between these points so that a continuous surface can be formed in a 3-D space. There are three main structures of DEM to model the earth's topography. These are:-

i. ***Gridded Structure*****:** Gridded DEM consists of regularly placed, uniform grids with the elevation information of each grid. Regular grid data structure is currently widely used for DEMs. It is simple to structure and compute, facilitating the automatic generation of photogrammetric and remote sensing imagery (Theobald, 1989). The GDEM thus give readily usable data sets that represent the elevation of surfaces as a function of geographic location at regularly spaced horizontally (squire) grids. Since the GDEM data stored in the form of simple matrix, values can be accessed easily without having to resort to a graphical index and interpolation procedures.

Accuracy of the GDEM and the size of the data depend on the grid size. Use of smaller grid size increases the accuracy. However, it increases the data size, and hence results in computational difficulties when large area is to be analyzed. On the other hand, uses of larger grid size may lead to the omission of many important abrupt changes at sub-grid scale (Theobald, 1989).

ii. ***TIN Structure:*** TIN is a more robust way of storing the spatially varying information. It uses irregular sampling points connected through non- crossing and non-overlapping triangle networks to simulate topographical surfaces. The vertices of the triangles match with the surface elevation of the sampling point and the triangles (facets) represent the planes connecting the points.

Location of the sampling points and hence irregularities in the triangle are based on the irregularity of the terrain. The advantage of a TIN model is that it allows stratified sampling of ground elevation. Where the terrain surface is flat, less sample points can adequately represent the surface. In rugged terrain, on the other hand, more sample points may be used to preserve details of the terrain features. Additionally, a TIN can take into account various topographical feature points (e.g., peaks, pits, and saddle points) and lines (e.g., ridges, valleys, and cliffs), allowing it to accurately approximate complex topographical surfaces from relatively few sampling points. A TIN, however, has its drawbacks. Its storage and management, and data manipulation process are relatively complex, costing significantly higher in computation compared with grids, particularly when a large dataset is used. TIN uses a dense network of triangles in a rough terrain to capture the abrupt change and a sparse network of triangles in a smooth terrain. The resulting TIN data size is generally much less than the gridded DEM. TIN is created by running an algorithm over a raster to capture the nodes required for the triangles. Even though, several methods exist, the Delaunay triangulation method is the most preferred one for generating TIN.

Due to its capability to capture the topographic irregularity, without significance increase the data size for hydrologic modeling under a certain circumstances. TIN DEM has been considered to be better than the GDEM by some researchers (Turcotte et al., 2001**).** Using TIN, flow path can be computed along the steeps line of descent of the TIN facets (Joneset al,. 1990).

iii. ***Contour-Based Structure:*** Contour represents point having equal height or elevation with respect to a particular datum. Such as Mean Sea Level (MSL). In the contour-based structure, the contour lines are traced from the topographic maps and are stored with their location(X, Y) and elevation information.

These digital contours are used to generate polygon, and each polygon is tagged with the elevation information from the bounding contour. The contour and flow path (i.e., the normal of the contour line) can be used to divide the topographical surface into irregular polygons, which can simplify the analysis and computation of hydrological models. This type of structure is, therefore, relatively common in hydrological modeling and related analytical geosciences.

Major drawback of contour-based structure is that the digitized contour gives vertices only along the contour line, whereas not many sampling points are available between the contours. Generally, the various topographical factors and features in DEM applications can be produced from each of the three DEM structures, although the grid DEM is the simplest, and relatively more efficient. Because of this, at present, DEMs have been commonly defined as grid structures (Theobald, 1989) and many countries provide DEM data only in the regular grid matrix format. Advantages such as the high degree of automation of data collection, the simplicity of computation and database management, and the ease of integration with remote sensing and raster GIS have given grid DEMs a dominant position in applications (Tang, 2000). Nevertheless, digital terrain modeling data structures are not static and a large number of algorithms allow for conversion between different structures of DEM. Therefore, in selecting data structures for digital terrain modeling, the data source, technical requirements, and the aim of application must be considered.

Finally, we conclude that the elevation data can be represented digitally in a gridded model where the point of elevation stored in regular grid, a triangular irregular network (TIN) and contours. Depending on these data structure, the DSM elevation data were generating by interpolating the regular grid from an irregularly distributed elevation data set or generating the grid directly using photogrammetric techniques.

2.3. Source of Digital Elevation data

Elevation information for a DEM or DSM may be acquired through filed surveys, from topographic contours, aerial photographs or satellite imageries using the photogrammetric techniques. Recently radar interferometric techniques and Laser altimetry have also been used to generate a DEM or DSM.

2.3.1. The Concept of Remote Sensing

The simple definition for the term remote sensing is "remote sensing (RS) is the acquisition of information about an object without touching it". In the other way remote sensing is the "non-contact recording of information from the ultraviolet, visible, infrared and microwave region of the electromagnative spectrum by means of instrument such us, camera, scanner, lasers, linear arrays, and/or area arrays located on plate form such as air craft, and the analyses of acquired information by means visual and digital image processing" (Jensen, 2007). In much of remote sensing, the process involves an interaction between incident radiation and the target of interest.

Remote sensing sources (aerial photograph, satellite images) are widely used for creating topographic map and digital elevation model. Remote sensing images of high resolution offers a rapid and cost effective means of extracting topographic and cadastral information for creating maps. Although, aerial and satellite surveys are not the best alternative to field survey with respect to surveying accuracy of positions in many countries. It is impossible to do mass rapid cadastral and topographic surveying, and RS techniques can be alternative approach for the establishments of topographic maps (Michael et al., 2016, Pp.41). Thus, according with General Survey Instruction Rules for British Columbia (GSIR, 2015**),** the position of natural objects may be determined by any survey method that yields accuracy of 0.5 meters or better. Such methods also can include indirect photogrammetric method e.g. aircraft and satellite images. In this method the scale, flight altitude of the satellite and air craft defined the desired resolution the DSM data.

2.3.2 The Concept of Aircraft Optical Imagery

Another way of airborne aerial photograph data has become a major source of digital terrain information. It is the art of capturing photograph of any landscapes, attributes or phenomenon on the surface of earth with the aim of building maps by using camera that may be placed on an aerial platform (Gilvear and Bryant, 2003). The primary focuses of collecting aerial photograph are producing orthophoto and terrain modeling. In 1858, from an air balloon Persia balloonist and photographer Felix Nadar captured the first aerial photograph. Historical mapping is about 9 x 9 inch. It is also a process of making of images from an aircraft (up to 50km) or balloon (or some other plate form) within the earth's atmosphere (Michael et al., 2016, Pp.41). Aerial photographs and digital aerial imagery has been a primary source of topographic and cadastral

mapping in medium and large scale for quite along a time. Aerial photographs started almost as soon as portable camera were invented and become practical with the invention of the airplane. As the camera was used more for aerial photographs, the science and profession of photogrammetry was defined. Digital aerial camera are replacing film camera as the sensor of choice in the 1990s. Aerial photograph is a passive method of RS which use's reflected energy from the sun. Two basic types of camera are used in aerial photography, aerial photographic camera and digital CCD (charge-coupled device) cameras.

A photograph refers specifically to images that have been detected as well as recorded on photographic film. Photographic films can be sensitive to light from 0.3 to 0.9 μm in wave length covering the ultraviolet (UV), visible and near infrared (NIR).

Digital cameras record electromagnetive radiation electronically and they differ significantly from their counterpart that uses film. Instead of using film, digital camera uses a gridded array of silcon coated. The CCD is a rectangular array of pixels that respond to light and record and the intensity of the range of the electromagnetive spectrum that it is calibrated to record. It is possible to split multiple CCD's across multiple lenses or use multiple CCD, s with a single lens to simultaneously record different portion of the electromagnetic spectrum.

Modern digital imaging systems are capable of collecting data with a spatial resolution up to 1.8cm at 300m flying height and with a spatial of four multispectral bands: Blue, Green, Red and Near Infrared plus panchromatic band (Michael et al., 2016, Pp.41).The size of the pixels array varies between systems, but typically ranges between 512×512 to 17310×11310 pixels. Radiometric resolution can be up to14 bit.

Due to the orientation of aerial camera respect to the target area, it deviate the accuracy of the image quality. So, depending on the orientation of the camera relative to the ground during acquisition when obtaining vertical aerial images, the aircraft normally flies in a series of lines, each called a flight run. The line is used to determine the position and orientation of the air craft. The distance the camera moves between exposures is called the air base which is used to determine the photo size. Aerial image are taken in rapid succession looking straight down at the ground and overlap within and between flight run in order to produce a stereoscopic view. On the other hand, the area covered by a single image and the over lapping of photographs may

affect the quality of the image. The overlap in these two directions is called forewarned overlap (end lap) and side lap. Forward overlap with in a flight run is from 60% to70% between sequential images. Side lap between flight run is from 25%-40% and ensures that no areas are left no photographed (Fig 2.1).

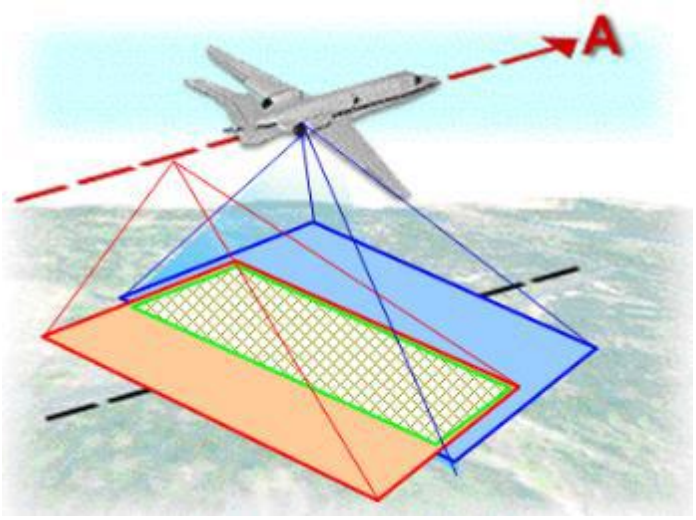

Figure 2.1: Illustration of flight run, airbase and overlaps (Michael, 2016)

According to Kennie and Petrie stated that in reporting (Hirt, 2015), Modern airborne and spaceborne sensors are considerably more efficient for terrain surface mapp ing than ground methods. This is because aerial photograph a larger area can be mapped more resourcefully and economically than traditional survey methods and can be used in areas that are unsafe and difficult to access. But, Weather conditions could affect the quality of the picture and the flight plan. Conditions such as snow might give a false representation of the ground, The ground that is usually hidden by structures such buildings or by tree canopies and vegetation cannot be accurately mapped, Accuracy of contours and cross sections depends on flight height and accuracy of ground control and Generally, aerial photogrammetry cannot produce the same level of accuracy as traditional survey field methods.

There are a few primary uses of aerial imagery: topographic surveying and mapping, digital elevation model extraction, visual and image interpretation and background use. The consideration of aerial image for a particular mapping application depends on the scale of imagery. The accuracy and photo map scale relationships mainly depends on the resolution of aerial images, the flight height, the base height ratio and of the stereo-plotting. Thus, aerial

images with spatial resolution less than 10cm can be used for mapping at 1:500-1:5000 scales' range.

2.3.3 Elements of Photogrammetry

Photogrammetry is the science of using aerial photograph and other remote sensing imageries to obtain precise measurements of natural and human made feature on the earth and produce plannimetric (topographic) maps (Michael et al., 2016, Pp.41). A photogrammetric technique provides continuous elevation data using pairs of stereo photographs or imageries taken by instruments onboard an aircraft or space shuttle. Radar interferometry uses a pair of radar images for the same location, from two different points. The difference observed between the two images is used to interpret the height of the location. Lidar altimetry also uses a similar principle to generate the elevation information.

There are four major phases in Photogrammetry which are directly related to the on-going advances in technology throughout the years especially with airplanes, electronics, computers and software. The first generation was the invention of photography. The second generation was the era of analog photogrammetry when photogrammetry is the science of determining the physical dimensions of objects from measurements on aerial photographs or imagery, was first implemented in 1849 using terrestrial photographs taken on the earth's surface (McGlone, 2004). In the 1950s the third generation was born with the invention of the computer. This phase was the Analytical photogrammetry generation. The fourth generation in photogrammetry is actually the current phase, called digital photogrammetry. In this phase the transition from analogue to digital began. Photography is transformed to digital data and photogrammetric processes are done by specialized software on computers. Digital cameras are now used, thus the photography is already in digital format and therefore there is no need for scanning. The main reason behind the push to extend analogue and analytical photogrammetry into the digital realm is for the expectations of huge cost savings in producing typical photogrammetric outputs and the new ability for using this digital output as input into other analysis systems rather than other surveying techniques. Photogrammetry is a skilled profession for the reason that obtaining reliable measurements requires certain skills, techniques and judgments to be made by the Photogrammetrist and experience is an advantage. It is a science and technology because it takes information from an image and transforms this data into meaningful results. Aerial

photogrammetry, which utilizes images taken from aerial or satellite platforms, followed soon after the first photographs were taken from aircraft. The process of photogrammetry involves three different components.

I. Image acquisition

Making the flight plan: - in this stage, decided the number of flight lines, their location, the spacing between them and their orientation depends on the characteristics of the project to be mapped. On the other hand, specify which outline how to take the photos, including camera and film requirements, scale, flying heights, end lap, side lap, tilt and crab tolerances, etc.

Selecting an appropriate camera system and camera size: - The camera is one of the most important types of equipment used in the photogrammetric process as it is the data in which all photogrammetric principles will be applied to. The camera should produce distortion free images in rapid successions in a moving aircraft. And also select image recorded stable film size.

II. Image control

This component is important because it is the control that is used to establish the position and orientation of the camera at the moment of exposure. Photographs can be controlled using three different methods. The first one is measured independent Ground control points which are surveyed by normal survey methods which is an integral part of photogrammetric mapping and should be carefully considered. The second is bridging control through aerial triangulation. This is done by computing on the photographs common points that appear in three successive photographs or in two adjacent strips and computing their 3 dimensional coordinate values. The last one is aerial photography control by kinematic GPS measurements; this will give the position and elevation of the camera without the use of ground control.

III. Product compilation

The product compilation varies and is dependent on the nature of the final product. Each of these components requires the utilization of different equipment, different measurement techniques, and different data processing. The most commonly used photogrammetric instrument is the stereo plotter. Its main purpose is to reconstruct the original orientation and the geometric integrity of an image at the moment of exposure and to collect three dimensional data.

A photographic image is created in a central perspective where it is assumed that every light ray from the earth surface reaching the plane of the film during exposure passes through the camera lens which is mathematically considered a single point, the perspective of the center of the lens. Photogrammetric accuracy depends on two main factors, the desired scale of the photography and the errors that are introduced during the photogrammetric process. The photo scale is dependent on the product specifications. The required accuracy can be met by using a small photo scale and high quality equipment or large scale photos with less accurate equipment.

The scale of a vertical photograph approximately equals the ratio of the flying height above the ground (H) to the focal length of the camera lens (f). The scale of a vertical photograph can be calculated as

$$\boldsymbol{scale} = \frac{\mathbf{f}}{\mathbf{h-N}} \qquad 2.2$$

With respect to scale and distance, image contains distortion inherited from a central perspective projection and distortions are different than those found on topographic map. When it comes to the photogrammetric product of an Orthophoto, the components that contribute errors to the product are: Camera (characteristics and calibration), Scanner (characteristics, calibration, resolution or image scale), Ground control (accuracy, distribution, and abundance), Aerial triangulation (design, measurement, and computation), Digital Elevation Modeling (DEM) - (method of compilation; quality of the source material; characteristics of the terrain; sampling spacing, with or without break lines; type of break lines used; method of interpolation into pixel grid and availability of height information on or above surface features, such as buildings.) and Rectification process (method and software) When all of these errors are propagated and summed up following a valid error theory methodology, one can assess the spatial accuracy of the final product. Geometric distortions are errors on an image between the actual image coordinates and the ideal image coordinates which would be projected theoretically with an ideal sensor and under ideal conditions.

Finally we conclude that the accuracy value of DSM data derived from photogrammetry surveying vary with scale and resolution of the aerial photograph; the flight height at which the photograph was obtained and the base to height ratio or geometry of the overlapped photograph. For example the scale between 1:5000th to 1:15000th yields a vertical RMSE value of 0.1-3m.

On the other study reported, the accuracy of DSM derived from aerial photogrammetry images produced a RMSE value of 0.1-1m. But the accuracy of DSM derived from remote sensing imageries that are; Radargrmmetry and SAR interfereometry yield a RMSE value of 10-100m and 5-20m respectively (Li et al., 2005). On other hand, data derived from contour interval, is the maximum permitted error are not greater than one-third of the contour interval. No errors are accepted which are greater than two-third of the contour interval. All remote sensing imageries (including vertical aerial and digital photographs, satellite imageries) are inherently subject to the roughness of the terrain surface, the interpolation function, interpolation methods and other three attributes of accuracy, density and distribution of the source data (Li et al., 2005). Due to the above accuracy reported in the previous studies, the accuracy value of DSM derived from photogrammetry source was a best way rather than remote sensing for great uses in the future either to create DSM or check the quality of DSM for terrain investigation.

2.3.4. Global Positioning System (GPS) measurement

Field surveys using like RTK GPS and Total Station were give the point elevation information at various locations. The points can be selected based on the topographic variations. Contours are the lines joining points of equal elevation. Therefore, contours give elevation at infinite numbers of points, however only along the lines.

A digital elevation model can be generated from the points or contours using various interpolation techniques like linear interpolation, kriging, TIN etc. Accuracy of the resulting DSM depends on the density of data points available depicting the contour interval, and precision of the input data. On the other hand, field surveying used for data accuracy assessment where the data collected independently.

As of today, the complete satellite technology is the GPS technology and most of the existing worldwide applications related to the GPS technology. The Global Positioning System (GPS or originally known as NAVSTAR) is a worldwide radio-navigation system formed from a constellation of 24 satellites and their ground stations to assist the position of geographic coordinate of a selected phenomenon (Michael et al., 2016, P.41). The GPS can be used to locate positions anywhere on the earth. Operated by the U.S. Department of Defense (DoD), GPS provides continuous (2 hours/day), real-time, 3-dimensional positioning, 46 navigation and

timing worldwide (Michael et al., 2016, Pp.41). Any person with a GPS receiver can access the system, and it can be used for any application that requires location coordinates. The first GPS satellite was launched by the U.S. Air Force in early 1978. The current GPS constellation consists of 24 satellites plus spares, located in 6 orbital planes, which are inclined 55 degrees to the equator. As of August 17, 2015, there were 31 operational satellites in the GPS constellation.

Each satellite orbits at 20,200 km altitude above the earth surface. This altitude defines the scale of the photograph. The orbits are very high so that they are stable and predictable. If the orbits were lower, friction from the Earth's atmosphere would eventually alter the orbit of the satellite. Each satellite orbits the Earth every 11 hours 56 minutes, which means that they pass over any point on the earth about twice a day. The satellites rise (and set) about four minutes earlier each day, and are synchronized with the celestial sphere.

Each GPS satellite is sending out signals with the following content: the satellite's ID, position and time stamp. In addition, each satellite sends a navigation message about the position of other satellites (ephemeris and almanac data) used in GPS receivers for later calculations and adjustment of errors. This content is modulated onto a carrier frequency signal in order to be sent from the satellite to the receiver. There are two basic kinds of GPS ranging codes (codes used to determine $propagation\ time$): these are Coarse Acquisition (C/A) and Precise (P) codes. C/A-code and P-code are used for the satellite clock reading, both are characterized by a pseudorandom noise (PRN) sequence. Current C/A and P(Y) code-signals are broadcast on both the L1 and L2 frequency carriers.

The GPS navigational message is used for prediction of orbital parameters and contains two different pieces of information – ephemeris data and almanac data. After turned on, a GPS receiver must update its almanac and ephemeris data and store it in memory. Ephemeris data tells the GPS receiver where each GPS satellite should be at any time throughout the day. After using all of these parameters, corrections to satellite coordinates at signal transmission time are calculated. Satellite coordinates refer to the WGS 84 system. Satellite almanac data are used by GPS receivers to predict positions for the satellites (ephemeris).

The Cartesian coordinate system of reference used in GPS/GLONASS is called Earth-Centered, Earth-Fixed (ECEF). ECEF uses three-dimensional X,Y,Z coordinates (in meters) to describe the

location of a GPS receiver or satellite. The origin (0,0,0) of Earth-centered reference is located at the mass center of gravity (determined through years of tracking satellite trajectories). The axes of reference are fixed with respect to the earth (that is, they rotate with the earth). The Z-axis pierces the North Pole, and the XY-axis defines the equatorial plane. GPS measurements are calculated by GPS software in the geographic coordinate system of WGS84 datum with Geodetic Reference System 1980 (GRS) ellipsoid (ECEF). Then, a receiver or office GNSS software like Lieca Geo Office can transform satellite coordinates to other coordinate systems, NAD83, УСК–2000, UTM, Adndan etc in order to produce DEM or checking the accuracy of any remote sensing data.

The height determined by GPS measurements relates to the perpendicular distance above the reference ellipsoid and not the elevation above Geoid or Mean Sea Level (MSL). So, GPS data needs transformation process in to a local datum of Geoid.

Finally, we conclude that GPS equipment has been considered as ground based acquisition technique that allows high accurate data measurements. It is not an alternative way of producing DSM data set due to inaccessibility of the continuous mountain area and low speeding and high cost consuming to measure the target area. Data collected by GPS receiver were giving the point elevation information at various selected geographic locations for the purpose of DEM or DSM data generation and/or used for checking the accuracy of DSM data independently.

2.3.5. Global Positioning System (GPS) errors

All measurements are not free from errors. To minimize the possible errors that occur at the observation, many researchers' studies and model the error sources of measurement. There are many sources of possible errors that would be degrading the accuracy of positions computed by a GNSS receiver (Michael et al., 2016).

The errors that can affect the accuracy of standard GNSS pseudo-range determination, is that ***Satellite clock****;* which is an error source occurred by the transmitted clock. Small variations in the atomic clocks (clock drift) on board the satellites can translate to large position errors; a clock error of 1 nanosecond translates to 3 meters user error on the ground. ***Orbit errors (ephemeris data);*** which is an Errors source occurred by transmitted location of the satellite orbit. Errors in the ephemeris data (the information about satellite orbits) will also cause errors in

computed positions, because the satellites were not really where the GNSS receiver "thought" they were (based on the information it received) when it computed the positions. ***Ionospheric delays;*** Atmospheric effects are the largest source of error that degraded the measurement. Because of free electrons in the ionosphere, GNSS signals do not travel at the vacuum speed of light as they transit this region. Delays in ionosphere can be compensated by using dual frequency receivers. ***Tropospheric delays;*** another deviation from the vacuum speed of light is caused by the troposphere. It is occurred by the variation in temperature, pressure, and humidity all contribute to variations in the speed of light of radio waves. Delays in troposphere can be only estimated the error source. ***Receiver noise;*** it is an error source which is distortion of the GPS signal caused by electrical interference or errors inherent in the GNSS receiver itself. Errors were occurred in the receiver's measurement of signal caused by thermal noise, software accuracy, and inter-channel biases. To minimize this error source, select GPS position which free from any receiver noise. ***Multipath;*** Errors caused by reflected signals entering the receiver antenna. The GNSS signal is a radio wave signal that can easily be blocked. Mountains, trees, towers, and buildings are just a few examples of possible obstructions. To reduce the possible obstruction, choose the observation point where points are free from this obstruction objects. The last one is ***Geometry of satellite positions;*** Errors are cumulative and increased by PDOP (Positional Dilution of Precision).

Finally, accuracy is one factor influencing the overall quality of measurements. To reduce the factor that degraded the quality of measurements, points are measured free from any disturbance of the GPS receiver.

2.4. Geographic Information System, GIS

GIS is a system in which software, hardware and events are designed in a way to assist the analysis, manipulation, management, capture and display of spatial data for the purpose of solving problems which are complex in nature. GIS can be implemented with customization in any organization. GIS deployment does not need any capability developed for different applications. It is generally a system which analyses, integrates, share and edit the information which is geographic in nature. It contains the tools which help the users to analyze spatial information and create the interactive queries (Scmandt, 2009). GIS is also the science which uses the geographic applications, concepts and systems. The major features of GIS depends upon

the two structures, first is the vector and the other is raster. Raster or vectors are denoted by layer of dataset. The raster file can be converted into the vector layer and vector layer can be converted in to raster layer. But this depends on the type of analysis being conducted with the data. There are information about the geometric properties and table of attributes in the each layer. Discrete features in form of lines, polygons and points are represented by the vector layers. They do not contain information regarding temporal or spatial data (Burrough and McDonnell, 1998). Continues features satellite and aerial imagery is represented by raster layers. They also represent the Digital Surface Models (DSM) through which elevation data across the surface are stored. Each pixel of thematic raster layer represents the attributes values. Physical values are represented by pixel value. The important functions of the Geographic Information System include the management of data base, spatial analysis and geo-processing and visualization and creation of maps.

i. Database Management

Storage, manipulation, creation and organization of spatial and non-spatial data are done by GIS database (Burrough and McDonnell, 1998). The geographic and non-geographic data is linked with each other through the GIS. Assessment of various data types is also done through database management. Comparatively Geographic data bases make explicit location distinctions for each data set which is being stored in data base (Arctur and Zeiler, 2004).

ii. Geo-processing and Spatial analysis

Spatial relationships can be calculated, analyzed and manipulated by the use of GIS. It can also be used to create the new data (DeSmith, GoodChild and Longley, 2007). Geo-processing can be termed as the manipulation of data sets such as extractions of new information using existing layers and clipping geographic content after the calculation of input layers (Wade and Sonmmer, 2006). It is central concept in GIS and contains more calculations which are complex and developed from methodologies that are outside of GIS and incorporated in to GIS overtime (Conolly and Lake, 2006). It can summarize and analyze the spatial properties of geographical distribution which can solve the problems of spatial data through the decision making (Longley et al., 1999).

iii. Data Visualization and Map Creation

GIS data can provide the researcher with the different type of formats which can enable them to create the updated links and relationships between the data of variety of links and relationships between the spatial entities. GIS acts as a cartographic platform which help in creation of maps, which can be done to present the geographical data or making analysis using spatial data. Maps using symbolizations and annotations display the result of GIS analysis (Michael et al., 2016)

GIS is a layer based like a map. Logical collections of individual features and geographic locations and shapes are represented by GIS. It also represents the information which is descriptive (Bolstad, 2005). The features which are stores are termed as attributes. The infrastructure of making maps and GIS is provided by the system through the community and across the web. Base map layers are introduced in GIS software. It provides map layer functionality designed to enhance rendering performance. Layers are drawn continually during navigation and it help in eliminating whitespace while editing and planning. The performance depends upon the back track caching and drawing engine (Elangoval, 2006).

2.5. The Concept of Positional accuracy assessment

From the very first days of aerial photogrammetry, positional accuracy has been assessed by comparing the coordinates of sample points on a DSM against the coordinates of the same points derived from a ground survey or some other independent source deemed to be more accurate than the DSM (Congalton and Green, 2009). In the early twentieth century, mapping scientists focused on map production and attempted to characterize each different contributor to positional error. Now, positional error assessment is more User-focused and emphasizing the estimation of the total error regardless of the source of data.

The first draft of spatial accuracy standard was established by the American Society of Photogrammetry (now the American Society for Photogrammetry and Remote Sensing or ASPRS) in 1937. Soon after, the U.S. Bureau of the Budget publishedthe *United States National Map Accuracy Standards* (NMAS) in 1941. The current version of the National Map Accuracy Standards was published in 1947 (U.S. Bureau of the Budget, 1947) and is included in the following text (Congalton and Green, 2009):

1. “Horizontal accuracy. For maps on publication scales larger than 1:20,000,not more than 10% of the points tested shall be in error by more than 1/30thinch, measured on the publication scale; for maps on publication scales of1:20,000 or smaller, 1/50th inch”.
2. “Vertical accuracy, as applied to contour maps on all publication scales, shall be such that not more than 10% of the elevations tested shall be in error by more than one-half the contour interval. In checking elevations the History of Map Accuracy Assessment taken from the map, the apparent vertical error may be decreased by assuming a horizontal displacement within the permissible horizontal error for a map of that scale.”
3. The accuracy of any map may be tested by comparing the positions of points whose locations or elevations are shown upon it with corresponding positions as determined by surveys of a higher accuracy. Tests shall be made by the producing agency, which shall also determine which of its maps are to be tested, and the extent of such testing.
4. To facilitate ready interchange and use of basic information for map construction: Among all federal map-making agencies, manuscript maps and published maps, wherever economically feasible and consistent with the use to which the map is to be put, shall conform to latitude and longitude boundaries, being 15 minutes of latitude and longitude, or 7.5 minutes, or 3.75 minutes in size.

The basic concepts of the report derive from the probability theories developed in the 1800s to predict the possible distribution of artillery shells fired at a target. It is opposite stand point compared to NMAS by proposing equations that should be applied to estimate the maximum error interval that would occur at various probabilities around the mean error. Relying on the root-mean-square error (RMSE) as the parameter to be estimated in characterizing positional map accuracy, the report became, and has remained, the foundation for all other publications that stipulate the calculation of map error from a set of sample points RMSE is the square root of the average squared differences between accuracy assessment sample map and reference locations (Maune et al., 2007).

The result was the 1998 publication of FDGC *National Standard for Spatial Data Accuracy* (NSSDA) (FGDC, 1998), which relies heavily on the ASPRS standards and “implements a statistical and testing methodology for estimating the positional accuracy of points on maps and in digital geospatial data, with respect to georeferenced ground positions of higher accuracy.” It

is also much-needed guidelines for measuring, analyzing, and reporting positional accuracy of both maps and georeferenced imagery such as orthophotos or ortho images. The standard explicitly does not establish threshold standards (as did the NMAS and ASPRS), but encourages map users to establish and publish their standards, which it was recognized would vary depending on the user's requirements.

Also relying on Greenwalt and Schultz (1962, 1968), the NSSDA specifies that positional accuracy be characterized using RMSE, requires that accuracy be reported in ground distance units at the "95% confidence level," and provides guidance on how samples are to be selected. NSSDA continues to be the accepted standard on positional accuracy assessment. It is often used in conjunction with the ASPRS large scale map standards, with NSSDA providing standardized processes for assessing positional accuracy and the ASPRS (1990) standards setting the maximum errors allowable for different map scales. The NSSDA standards have been widely accepted by many local and state government agencies, as well as by the private sector.

More recently, three new guidelines have been established for assessing digital elevation data. All three call for the stratification of positional accuracy assessment samples into land cover types. Two of the guidelines also mandate that accuracy be reported at the "95th percentile error" in addition to the NSSDA statistic.

FEMA's *Guidelines and Specifications for Flood Hazard Mapping Partners* (FEMA, 2003) adds a new dimension to positional accuracy assessment by requiring that a minimum of 20 samples be collected for each major vegetation type of which there may be a minimum of 3, resulting in a minimum of 60 total sites sampled. On the other hand *ASPRS Guidelines for Reporting Vertical Accuracy of Lidar Data* (ASPRS, 2004) ratify the FEMA guidance to stratify the landscape into different land cover classes. The ASPRS classes differ slightly from the FEMA classes. The National Digital Elevation Program (NDEP) *Guidelines for Digital Elevation Data* (NDEP, 2004) essentially mirror the ASPRS (2004) lidar guidelines for vertical accuracy reporting in calling for the computation of Fundamental Vertical Accuracy, Supplemental Vertical Accuracy, and Consolidated Vertical Accuracy. Finally, we conclude that the last Guidelines and Specifications that is ASPRS (2004), NDEP, (2004), and FEMA,(2003) were the most widely accepted standard guide line used for assessing of the vertical accuracy assessment of spatial data.

CHAPTER THREE

3. Materials and methods

3.1. Description of study area

The study area is found in the region of Addis Ababa, Ethiopia one of 10th of the major sub city which are selected to evaluate the vertical elevation derived from aerial photograph images in the city. The positional coordinate of the site lies between 38˚ 40' 00"−38˚ 47' 00" E and 08˚54'00"−08˚57'41.76"N (Fig 3.1). Its boarder surrounded by a districts of Kolfe_Keranio in North West; Lideta in the North; Kirkos in the North; Bole in the north East, Akaki_kality in the South East and Regional state of Oromiya to the South West (AACA, 2010).

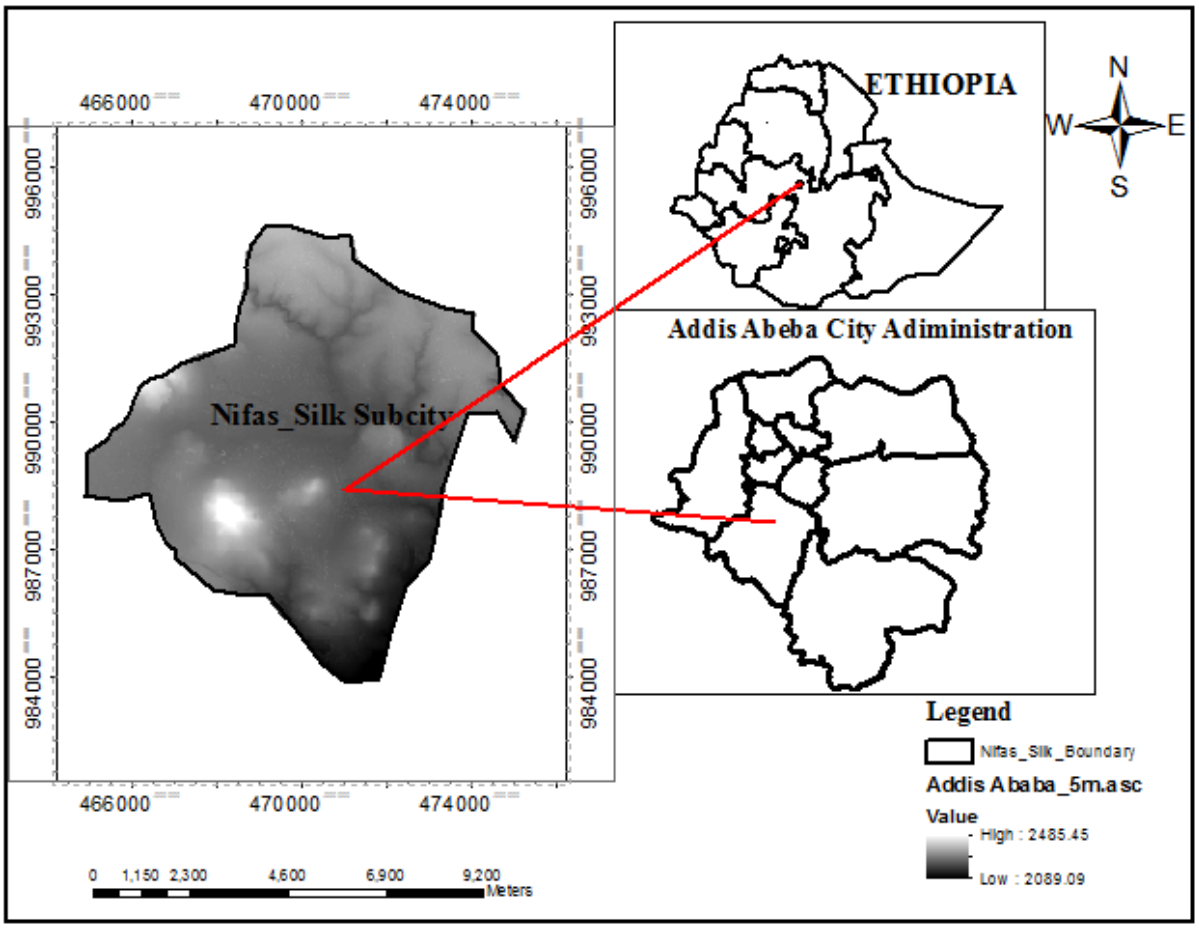

Figure 3.1: Location map of the study area

The sub city was divided in to twelve wereda and the total population and total area are 335740 and 68.30 km^2 (26.375sqmi) respectively. Nifas silk sub city is situated high plateau at the south west from the central part of the sub-city and flat at the central part of the sub-city. It exercised a number of land use activities such as, urban agriculture, residence, commercial, roads and rivers. It has with an altitude ranging from 2075 to 2488 meter above the Mean See Level. Most part of the urban area covered by gentle steepness topography.

3.2. Background of the data

3.2.1. Aerial Photograph DSM

Aerial photograph is a passive method of remote sensing which is used to producing an image using reflected energy from the sun. Airborne photograph was one of data acquisition method produced two products that are orthophoto and Digital Elevation Model begins with digital photograph or video taken from a camera mounted on the bottom of an air plane. So it has taken overlapping photographs or video of the entire area to get complete coverage of the project area. Images area recorded in either analog (physical or digital form). Digital images are recording in softcopy and record the radiance of the objects numerically in small, regularly spaced area elements. These values are stored as matrix format. According to Weitkamp stated that in (Fujii and Fukuchi, 2005) the distance rage between the camera and the target is calculated by multiplying the speed of light by half of the time it takes the light to travel from the camera lens to the target and back**.** The GPS receiver is used to recorded the aircraft time of the exposure and the IMU measures the altitude of the aircraft (roll, pitch, yaw or leading) (Webster and Dias, 2006)**.** The calculated range between the camera lens and the target object, gives us the position of the aircraft and its orientation information obtained from GPS and IMU which are used to calculate three dimensional spaces of the target features (Wehr and Lohr, 1999). The three dimensional aerial photograph DEM data are initially represents the latitude, longitude and ellipsoidal height based on the WGS_84 reference ellipsoid. It may be transferred the data from ellipsoidal height to orthometric height based on a national or regional height datum (Liu et al., 2007).

For the purpose of DSM generation, the accuracy of existing GCP point were a critical for triangulation which points are given connected by edges that form triangles approximating the shape of the terrain. This is often called a TIN (Triangulated Irregular Network) model. Some

algorithms have developed for automatically extracting ground points from all recorded DSM points.

The first digital line map of Addis Ababa were collected and organized in 2003-2004, which is prepared by Canadian company namely nortech using door to door field survey method. After six year later Hansa Luftbild proposed a technical flight mission to use a new aerial photography to update and coverage of Addis Ababa. This digital aerial photography is acquired at ground resolution of 0.2m and 10m by 10m vertical resolution. This resolution is suitable for mapping at scale of 1:2000 as well as to produce a digital orthophoto at ground sample distance (GSD) of 0.20m (Gizachew, 2012, pp.2). To relate the coverage of pre-planned flight lines to the location of photo control points all planning activities were based on the SRTM90m digital terrain model (Gizachew, 2012, pp.2). After receiving the border of AACA, individual photo control were pre-computed in WGS84-coordinate, representing the coordinate system of GPS and were convert to Adindan datum. The flight direction was planned to run in east-west or west-east direction and 60% at forward overlap and 30% at lateral overlap.

Hansa Luftbild uses VexcelUltraCamX camera system. This camera system delivers radiometrically and geometrically superior large format aerial imagery. The supports minimize the degree of errors, reducing cost and sensitivity to environmental effects. Due to this reason, the flight date was conducted 28th November and it was resulted 505 images. The flight height of the aircraft was about 2770 meter above the terrain surface and vertical resolution of 10m for mapping at scale of 1:2000 (Gizachew, 2012, pp.2**).** The second type of data which is conducted by INSA to cover the total area of Ethiopian country at the date of March 2016 at a ground resolution of 0.25cm and an approximate scale of 1:48088. This data have been collected from an average elevation of 2600m above terrain surface and produced a 10m by 10m vertical resolution. The levels of accuracy required for cadastral mapping depend on the source of the data. Based on the national standard adopted by EGII, the vertical accuracy levels in RMSE that must be achieved from aerial photograph were not exceed three pixel size of ground sample distance (in z). Both DSM data collected from EGII were represented with a sparsely distribution of the reference check point (See fig3.2 and fig 3.3)

3.2.1.1. Image Post-Processing

Both of the images were compressed in LAS format without loss of the original data quality. This data format exported in Arc ASCII Grid format using Global Mapper 1.8 and then processed the data in Arc GIS software package for the extracting elevation point to be accessed. Global mapper is an affordable and easily-to-use GIS data processing application that offers a variety of spatial data sets and provides right way GIS functionality for the extra processing of the data. It has a capability of elevation analysis such as querying, raster calculation, and contour generation from surface data, triangulation and gridding of 3D point data.

After collecting the data format, export the data in Arc ASCII Grid format command. The export Arc ASCII Grid command allows the user to export these elevation LAS data sets to an Arc ASCII Grid format file. After exported LAS data, the command displays the Arc ASCII Grid export option dialog which allows user to set up the exported data. The dialog consists of a general option panel which allowed the user to set up the Grid spacing and vertical units, Gridding panel and an export bounds panel which allowed the user to set up the portion of the loaded data for wish to export (Fig 3.2). Because, it is simple to structure, and compute, facilitating the automatic generation of photogrammetric and remote sensing imagery.

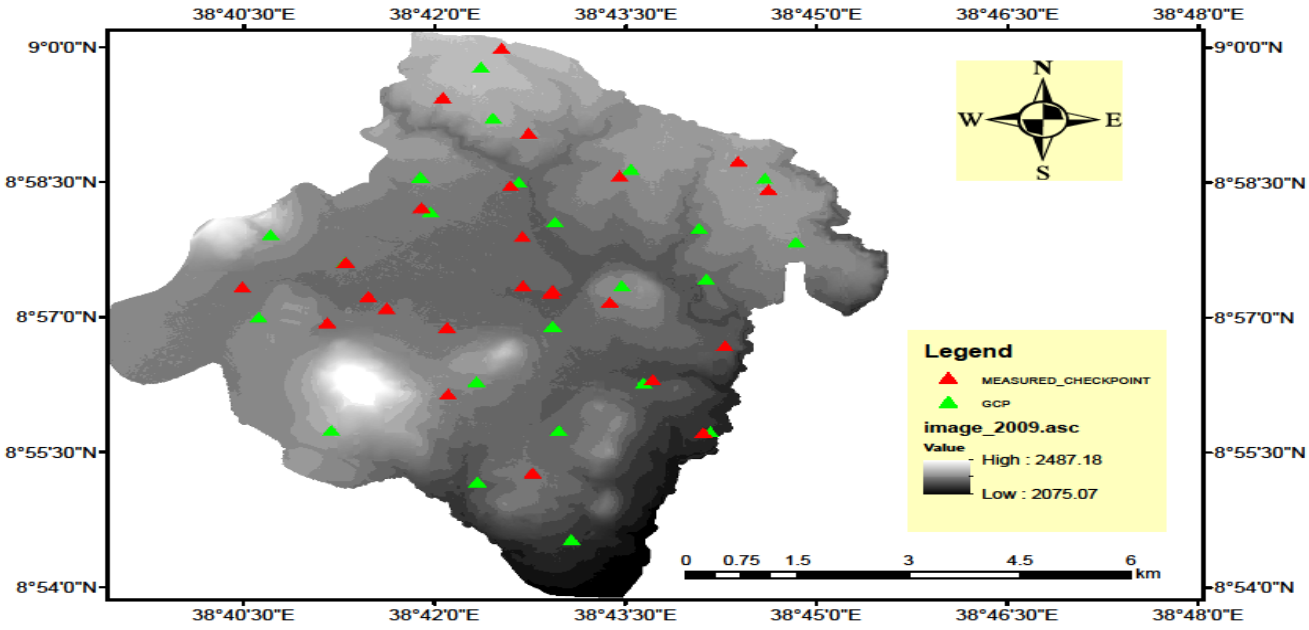

Figure 3.2: DSM (2016) data and Reference point.

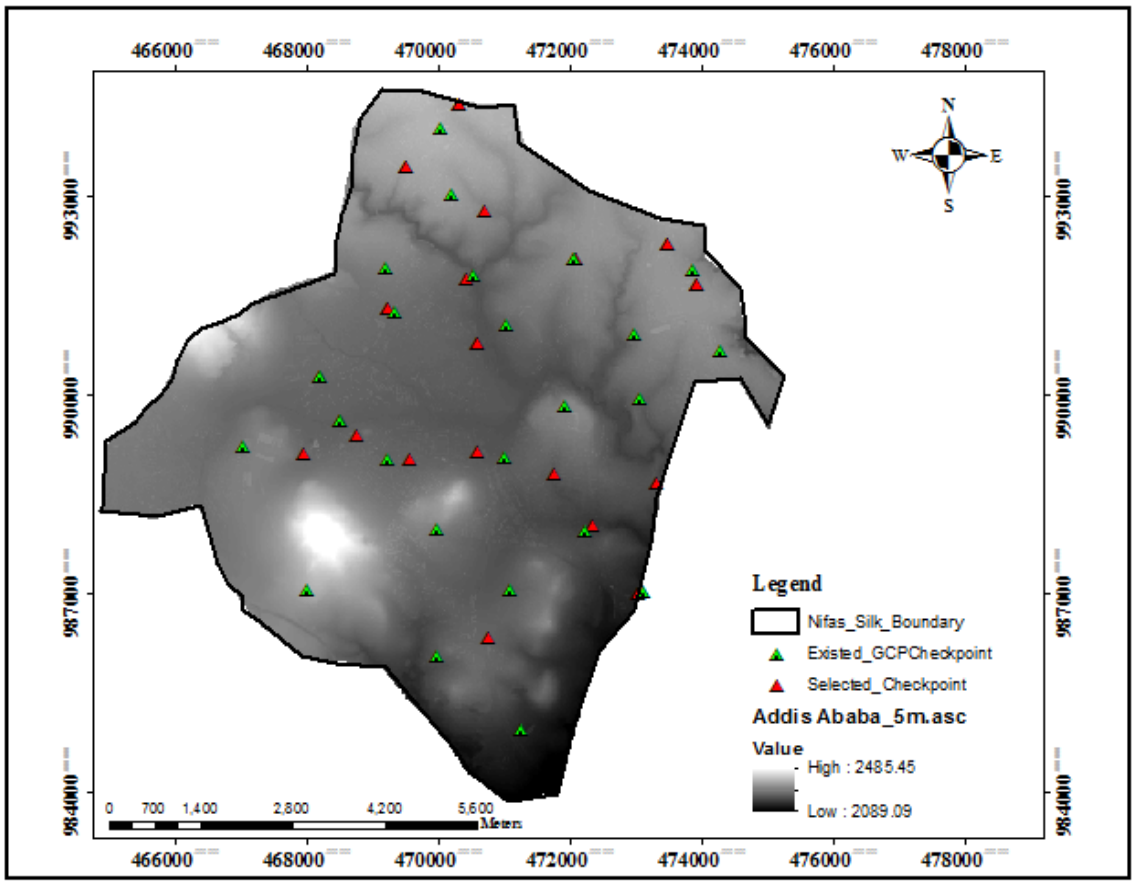

Figure 3.3: DSM (2010) data and Reference point

3.2.2 Ground Control Points and Suitability for Checkpoints

Geodetic control surveys are usually performed to establish a frame work of positions that provides a common reference system for establishing the coordinate of all special data (FGDC, 2008). Ground control points are the basis of the checkpoints and an important component of the spatial data infrastructure (Fig3.3). They have a physical position on the ground and their associated metadata, which have precisely measured horizontal and /or vertical location based on the national horizontal and vertical datum. In Ethiopia, the Ethiopian mapping agency is responsible organization for the establishment of the ground control points with the international coordinate system. For the purpose of building cadaster, City Government of Addis Ababa Integrated Land Management Information System Project Coordination (AACA) and the Ethiopian Geospatial Information Institute (EGII) established a contract agreement for the establishment of 555 (580 submitted and 88 are in Nifas Silk from the total) ground control points in Addis Ababa city in July 2011. The data were established sparsely distributed in

hundred meter of radius and visible each other. According to the agreement, the monuments of the GCP were established by AACA and EGII provided support in the selection of size and supervision task for the construction of monuments. The major tasks of EGII were observing the GCP, preparing, processing and submitting the necessary data to ZAACA. Those data measured for the production of orthophoto and digital surface model of the city. The station description for each of the GCP point in the sub city were constructed a concrete monument covered with and projected approximately 0.30m above the ground and it's center has marked by an iron bar (Fig 3.4). For the establishment of the GCP, EGII were planning and preparing the necessary equipment, the reference system observation techniques and observation time length. This survey marks was produced based on the reference system of UTM Zone 37N Projection System, Clark 1880 (ellipsoid), Adindan Reference Datum and EGM96 Height reference. The other planning of the EMA, conduct the survey mark uses Six Dual Frequency Geodetic GPS receivers (four Ashtech and two Leica 1200 brands) for the measurement of GCP point. This was achieved by static observation of a minimum of 1 hour or in the case of kinematic observation an antenna swap. Static GPS is a differential positioning method which provides centimeter accuracy for GPS baseline. According to the EGII, determine the accurate position of the new control point in the project by connecting to the 19 national points. The value of the primary control point coordinates was determined in 48 hours observation and their data were processed in connection with IGS points. The second order GCP were observed in 24 hours connection with the first order points and processed by Ashtech solution precession GPS surveying software. To obtain the required accuracy, EGII uses list squire adjustment processing software. They were established a horizontal accuracy of 0.020m+1ppm and vertical accuracy of 0.04m+2ppm at confidence level of 95%. Linear units of measure were in meter and the accuracy for the instrument as stated by the manufacturers is 5mm±0.5ppm. In these survey marks, the selected references GCP have a maximum deviation of 7.9cm in the horizontal and 18.1cm in the vertical.

Figure 3.4: Sample of GCP point description source (AACA, 2011)

3.3. Data Acquisition and materials

3.3.1. Static GPS Control measurement

Static observation is a method which provides a very high accuracy of points for GPS baseline (Keplan and Hegarty 2006). It is the most preferred approach for establishing the most accurate positions, the control. In static GPS surveying, the receiver was motionless for a time, usually a relatively long occupation. For example; some processing and data checking should be performed on the daily basis during a GPS/GNSS project. Blunders from operators, noisy data, and unhealthy satellite can corrupt this project.

Nifas silk sub city have a number of ground control points that was distributed across the whole area of the study. Before observing the static data, carefully planned and select five existed GCP point elevation for evaluating the accuracy the existed GCP point elevation in the study area. In this case, these reference stations were selected randomly for accuracy checked depending on the problematic condition of the topography. They are free from observation noise such as multipath; error estimated that distorted the original signal through interference of reflected signal from objects surrounding the receiver antenna where station of the receiver found. To reduce this error type; select the observation stations with no reflected objects in the vicinity of the receiver antenna. Atmospheric effect; the altitude and thickness of the atmospheric and ionosphere layer have changed the signals that transmitting from the satellite position to the base station. To reduce the probability error in the point station, observations were performed at obviously the same conditions at early morning and in the free sky. And also selected the point of position where points free from near building and long tree. After proposed and selected the GCP points, measured checkpoints were found at Jemo_ Condominium, Gebrael_Bridge, Michael Bridge,

Lafto_Maruta and Korie_Mekelakeya in the sub city of Nifas_Silk. Then, with LEICA_VIVA GS-14 receivers' techniques, coordinate of the GCP point elevation were performed in a static sense. These point elevation were observed for two days (from 11/11/2018-12/11/2018 G.C) in static mode for one hour extended period of time.

With Leica viva GPS receiver's techniques, set out the tripod and GS receiver over each base station with known location and configuring the static session as a fixed static reference point. In the GS receiver, the viva system is an ability to store the static GNSS observation directly to SD memory card. In the GS receiver, SD memory card were stored the row data in the form of leica MDB format files within an hour interval. After collected the static data in a set time needed, shutdown the GS receiver. Then, the file is closed and saved when the receiver is in the process of powering down from operation.

3.3.2. RTK GPS Leveling Measurement and Point extraction

Differential real-time positioning required a data link between the base station and rover. By connecting reference base stations with a rover points which were geographically distributed throughout the study area received GPS signals and forwarded them to the base station. Baseline vectors were produced from the antenna phase center (APC) of a stationary base receiver to the APC of the rover antenna using the X,Y,Z Cartesian coordinates of the ground control point with a reference datum of Clarke 1880 (ellipsoid) and Adindian reference datum, which is the reference system of Ethiopia. Global Positioning System (GPS) system broadcast orbits were realized (differential X,Y,Z vectors in other reference frames would be possible if different orbits were used). Since the location of the reference base station are correctly known, the base station (control) could be accurately calculated the check point position. The absolute accuracy of the rover's would be depending on the absolute accuracy of the base station or GCP point and the separation between base station and rover position (ICSM 2008). So in our measurement, the base line separation between the station and the rover on the checkpoint was visible and not greater than hundred meter from each other. At the beginning of survey work, a spatial configuration of the proposed checkpoint should be examined using ortho photographs. This is necessary for a researcher to plan where to set-up checkpoint station with RTK GPS and base station to measure the checkpoint elevation. Positions of the checkpoint station have to be selected according to the natural characteristics of the study area i.e. shape, terrain, building and

roads. In this project, the checkpoint selected on the building land use covers and fixed in open areas from which the point were clearly visible to the satellite receiver.

The Real Time Kinematic (RTK) measurement method involved using Eight existing GCP point as base station and one moving rover which are 24 receiving points were measured in the study area. The sample of measured points were also considers the position of GPS satellites in the sky. Measuring the sample point were free from any surrounding objects, such as building, trees, which have disturbed the GPS; signal received by a GPS device during the measurements.

There are many sources of possible errors that degraded the accuracy of elevation data during at GPS received in the area of the project. To avoid systematic and gross error, take an action in the time of measurement. Some are: satellite clock; to minimize the error at the check point, received the data when satellite signals of accurate time dilution of precession data transmitted. Atmospheric effect: - the check point of a research measured in the time of summer when weather condition was early sunlight day time for acquiring good satellite signals. Receiver noise: all check point position have been selected where, the points are free from electrical interference. Multipath: The sources of this error were very large in our measurement. We need to minimize the error where sample points were selected free from any disturbance of GPS signals.

Lieca RTK GPS receiver was used for GPS leveling measurements. To start the measurements at the station a new job was created on the base station. When a dialog of the new job was opened, the new job title was entered on the control device for example ‘Jemo 51’, ‘Lafto_Maruta’. Then, by pressing *contin* button metadata for control station can be entered. And also, the antenna height of the base station entered. Because, antenna height of receiver was on the base station affected the elevation leveling measurement. By linked the base and robber receiver, returning to the main menu and the survey option was selected.

The accuracy of ongoing RT leveling measurements of vertical coordinates was less than 0.03m. To achieve such accuracy, a high quality signal should be a waited for about 1-3 minutes. In addition, the PDOP parameter was considered when leveling measurement was performed. This parameter was show the accuracy of satellite signals, which was not exceeding 4.00 PDOP value. The smaller value of satellite signals was indicated the more accuracy of point coordinates given.

In this project, all 24 check points elevation were measured when error of GPS device was less than 0.03m and PDOP less than 4.00.

Where using the coordinate of the reference and their orthometric were known, determined the transformation parameters which allowed the ellipsoidal heights generated by GPS measurements to orthometric heights for the new checkpoints. In the reference point, there were orthometric heights with these points we can determined the three parameters of the checkpoint coordinates by one dimensional transformation methods. The plane coordinates of a known point of heights which can be interpolated on GPS measurements. At these points the undulation of the geoid does not have to be known when using the way of approach in transformation of heights. The undulation of the geoid in the new checkpoints was obtained from the reference point data by a linear interpolation. So, no need of transformation of reference datum which was compatible to the examined data.

After making the RTK GPS leveling measurement of the checkpoints in the study area, the raw data were transferred in to GIS software, where data processing to be performed. The software of lieca devices (GS receiver) includes a function of data conversion and export. In the main menu, click c*onti* button in GS receiver memory. Then the survey raw data were downloaded and export in .csv format. Using memory card reader, checkpoints raw data were transferred in to personal computer.

Using Arc GIS desktop, navigated .csv format of raw data in the file menu. To add a GPS raw data of x, y, z coordinates to a map layer, the raw data must be contained three fields: x, y, z coordinates. For making spatial information as a layer, added the x, y event layer tool from raw data that exported in .csv file format. The ArcGIS Spatial Analyst extension provided a rich set of spatial analysis and modeling tools for both raster (cell based) and feature (vector) data. After making the raw data as shape file, extraction of the examined data was performed corresponding to the checkpoint for statistical analysis. According to Wade and Sonmer, 2006 stated that geo processing can be termed as the manipulation of data set such as extraction of new information using existing layers and clipping geographic content after the calculation of input layers. The extraction tool allowed extracting from the cell value of a specific location of examined DSM data by attribute point feature class of the checkpoint. Finally, the output field names are created from the name of the input of DSM data by default to store raster values. The reference point

data and the point of the corresponding extracting examined both DSM data were analyzed in the next chapter.

3.3.3. Leveling measurement

Another method of checking the accuracy of both DSM was differential leveling techniques. It is a process of finding the height new point or points by comparison with that of an existing point which has been selected as a control network or whose height was already known with respect to some other datum. In this method a horizontal line of sight is established by using a sensitive level bubble in a level vial. The most common ground base methods to determine elevation were through the use of 1) a compensator type, automatic (engineering level) and level rod(s), and 2) an electronic digital barcode leveling instrument with barcode rod. The method that used to use in this research was rod leveling technique. Rods leveling are, in essence, a tape supported vertically, and used to measure the vertical distance (difference of elevation) between a horizontal line of sight and a required point above or below it. For comparison with other points, the scheme of leveling should be tied in to one or more nearby benchmarks of known heights. In this research, ten positional points were proposed with five reference benchmark of known points. These positions of checkpoint elevation have to be selected according to the natural characteristics of the study area, distance from the control station and points where RTK GPS checkpoint were performed which have used to generate the X and Y coordinate for extracting the examined data. After proposing of the position of the point, a simple process of differencing was done with a level and graduated staff. For performing a leveling, first, set out the tripod on the unknown height of the point near to the reference point. A level was a telescope mounted on the tripod, fitted with cross hairs and sensitive bubble; means were provided for setting the line of collimation (the sighting line) to be exactly horizontal. A staff was simply along a ruler and was usually graduated in centimeters.

To find the difference in level between the reference station and the checkpoint station, the observer set up the instrument at any point where it was at a maximum distance of 50m between the control stations and extending the observation of others using the same distance until reached at the checkpoint. An assistant holds the staff vertical with its foot resting on the benchmark of known points. It was known as back sight (BS) observation which was used to calculate the height of the instrument (HI). The observer rotates the telescope about its vertical axis until the

staff appears in the typically a horizontal v-shaped float in to a vertical wall. They were used by inserting a bracket in to the slot and standing a staff on the bracket. This bracket was a benchmark center of the field view sets the line of collimation to be horizontal and then reads the scale of the staff against the horizontal cross hair. Then sketched and recorded in notes, a field book or a data collector. The numbering or identification system should be consistent with district numbering convention, if any and should be identified with enough detail for another crew to locate the bench mark easily. The staff was then moved to another unknown station and the observer again directs the telescope on to it, obtaining the reading of foresight observation (FS) of unknown points. Successive rows of entries on the form refer to successive *staff* stations; the foresight and the back sight were therefore booked on the same line. The sight length between back sight and foresight should be approximately the same. At each instrument station, the height of the line of collimation is obtained from the back sight is added *(using Eq; 3.1)* and then reduced the level of the next foresight was calculated by subtracting the relevant staff reading *(using Eq; 3. 2)*. A booker, who may well also be the observer, books each reading in the field book as it was taken, using a pencil or ball-point pen. Fill in a name for each staff station; the entries in the distance columns need only be approximate and can be judged by pacing. If the height of the checkpoint were beyond to the reference station required, the instrument and the graduated staff were moved by repeating this process until reached to the selected checkpoint elevation obtained. This process was performed, when the staff was moved, the instrument must remained stationary, and when the staff remained stationary, and the instrument must move to guard against a reading error going undetected (Fig 3.5). By using a mathematical formula, all the entire elevation leveling process was calculated (using Eq; 3.1 and 3. 2).

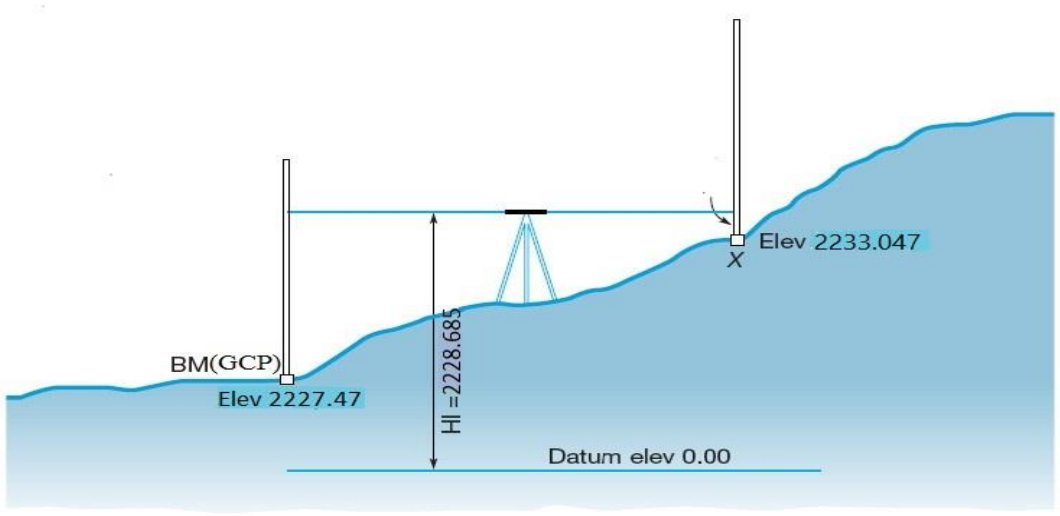

Figure 3.5: Process of differential leveling method (Lantek Eng. Consultant, Hyderabad)

After making all the necessary checkpoints elevation in the study area, prepared a raw data (X, Y, Z) and were transferred in to GIS software, where data processing to be performed. In this case follow the steps of data extraction of the examined data which explained in the above RTK GPS raw data processing steps (See figure3).

$$HI = BM\,(GCP) + BS \quad (3.1)$$

$$BM(x) = HI - FS \quad (3.2)$$

The above relationship was used for process of finding the desired elevation of a point. Where BM is the reference elevation respect to the datum at the starting and ending measured checkpoint, BS and FS stands for the back and fore sight of the relevant staff reading and HI is the height of the tripod plus the starting bench mark elevation. Using these relationships, field observations were conducted and analyzed the row data in the next chapter.

3.4 Methodology of the study

3.4.1. Data preparation

Elevation value collected from the reference point of existed GCP, static GPS measurement, RTK GPS and leveling measurement are compared with both DSM derived from aerial photograph. In this case the data measured by RTK GPS and leveling technique were depended on the existed GCP. In order to strengthen the acceptance of elevation accuracy, we must be evaluating the elevation accuracy of the used existed GCP point independently using static

measurements. Geodetic coordinates (latitude, longitude, ellipsoidal heights) are determined at every leveling bench mark using static differential GPS measurements. Both of the data should be transferred in to the same vertical coordinate datum. Before transferred the data, we must adjust and predicted these static observation with IGS service which used as a control or reference point (see figure 3.6). IGS was connected by the GPS navigational message which was used for prediction of orbital parameters and contains two different pieces of information; ephemeris data and almanac data (Keplan and Hegarty 2006). Each satellite transmitted a navigational message about the position of other satellites (ephemeris and almanac data) which have been used for further processing and adjustments. Ephemeris data could be used to accurately calculate the location of a GPS satellite in a fixed time of measurements. The data was recorded in ADDIS which is point of networked GPS satellite trucking used to adjust the week raw data of field static measurements. In this thesis static data measurement was performed for a length of two days. Each station of the point observed in a static sense was not greater than 20km from the IGS station of ADDIS. The transmitted navigation message was recorded and organized a week number of IGS 20093.SP3 and IGS 20094.SP3 format. After completed the fieldwork measurement, import the GNSS row data and ready to process the static data in Leica Geo office 8.4 (LGO). The static data for the GS base receiver is on the SD card used in the GS base receiver. Using this processing software, latitude, longitude and ellipsoidal coordinate of each station on the respective time of IGS network i.e. ADDIS data were computed with reference to WGS84 reference ellipsoid. In order to adjust the static row data IGS control station data was downloaded from http://igscb.jpl.nasa.gov.,When there was recorded at the day of measurement were performed (See Fig 3.6). The GNSS raw data was located under the /DBX directory of the SD card used in the GS base receiver, Each GNSS raw data file (.m00) was named with the last four digits of the serial number of the GS units, the data and time of file creation. Next create leica Geo office project and import the GNSS raw data and the IGS Ephemeris data in this project.

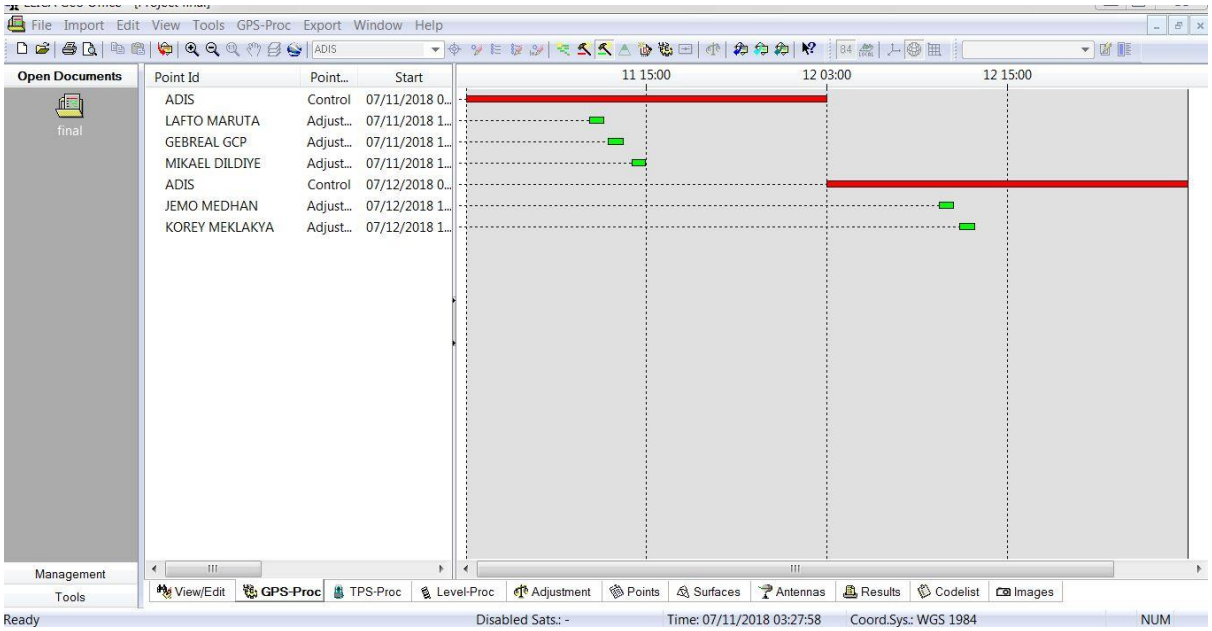

Figure 3.6: Post processing Solution for Five Control Points by using Lieca Geo Office Software

Two row data of the IGS point was used to adjust the five measured row data. Then right mouse-click on the point ID and choose properties… to observe the information from the static session. In the GPS process session, select "ADDIS" as a control or reference (red line color depicted in fig: 3.6) and the five measured raw data as rover (fig: 3.6 yellow line color) and then process the data to get the point data of the observation. After adjusted and predicted the row data of static measurements the data set was summarized in table3.1.

Table 3.1 Processed solutions of five control points using lieca geo office software

Point Id	Point Class	Date/Time	Latitude	Longitude	Ellip.Hgt(m)	Posn+Hgt.Qlity
JEMO MEDHANILEM	Adjusted	01/13/2019	8°57´ 15.66111´´N	38° 42´ 51.59752´´E	2220.9963	0.0109
KOREY MEKELAKEYA	Adjusted	01/13/2019	8° 58´ 30.23218´´N	38° 43´ 14.42938´´E	2254.4375	0.0270
GPS0031	Control	07/11/2018	8° 57´ 55.98843N	38° 43´ 38.42995´´E	2220.7010	0.0123
MIKAEL DILDIYE	Adjusted	01/13/2019	8°57´ 55.99573´´N	38° 43´ 38.43637´´E	2231.0419	0.0139
GEBRAEL DILDIYE	Adjusted	01/13/2019	8° 57´ 19.34745´´N	38° 43´ 57.31524´´E	2215.4570	0.0155
LAFTO MARUTA	Adjusted	01/13/2019	8° 56´ 57.00906´´N	38° 44´ 12.95800´´E	2210.8990	0.0148
ADDIS	Control	07/11/2018	9° 02´ 06.48703´´N	38° 45´ 58.69249´´E	2439.1558	0.0123

These point data reported in a coordinate system of WGS_84 ellipsoidal height reference (see Table 3.1). So, we must transform in to the local datum reference of the study area. The processed WGS_84 coordinate system of five sample data set observed in static sense presented in (Table 3.1).

From the above table 3.1 presented were processed and adjusted row data of static GPS observation. These row data was tabulated in geodetic WGS_84 reference system so, we should transform the row data into national local datum. In Ethiopia, Clark_1880 ellipsoid was used as a reference system which is mathematical earth shape used for processing the coordinate of Adindan (Ethiopia) Datum. It was generated the geodetic height of the ellipsoid. It is simply a minimum distance between the user and the reference ellipsoid. As explained in the above, the observation data reported in WGS_84 reference system. So, the data was changed in a local datum of Adindan (Ethiopian).

Based on the national standard adopted by EGII coordinate shall be calculated in referenced to grid on UTM projection and zone 37 depending of the geographical location and the datum transformation parameters provided by EGII shall be used for transforming the geodetic coordinates from WGS_84 to Adindan geodetic datum. In cadastral surveying and mapping activities the used transformed coordinates and translational transformation parameters adopted by EGII were as follows.

Semi major axis (a): 6378249.145m	$\Delta X = -162$
Semi_minor axis (b): 6356514.9667m	$\Delta Y = -12$
Ellipsoidal flatting (f): 1/293.466307656	$\Delta Z = 206$

Using the above transformation parameter, the used elevation must be transferred in to Adindan EGM96 Geoidal model.

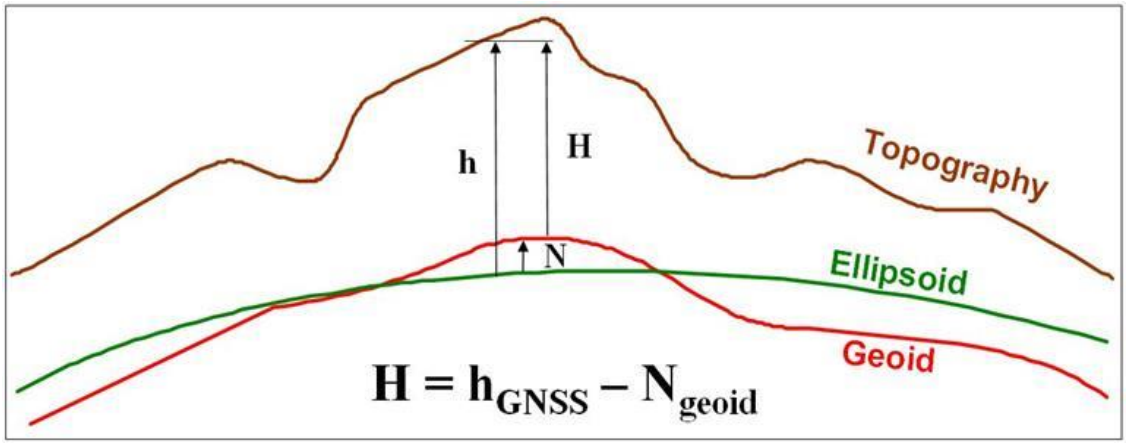

Figure 3.7: Ellipsoidal, Orthometric and Geoid heights (Roman.B PLSC, 2007)

The following relationship was used to transform elevation from ellipsoidal height to orthometric elevation:

$$H = h - N \qquad 3.3$$

where H is orthometric height, h is WGS84 ellipsoid height, N is EGM96 geoid undulation.

From the above relationship the ellipsoid height (h) was the height of a point above the surface of ellipsoid (from green line color in Fig. 3.7). Ellipsoid height was easily calculated from Cartesian EFEC coordinates. The Geoid height of (N) was the height above or below the ellipsoid (Red line color depicted in Fig 3.7). It was a complex surface, with undulation that reflects topographic, bathymetric and geologic density variation of the earth. In our measurement tabulated in table 3.1, the Geoid height was varying from -7.4701 up to -7.6309m inward of the ellipsoid. Geoid height is modeled and tabulated by geodetic agencies. The best known global geoid model is the National Geospatial -Intelligence Agency/National Aeronautical and Space Administration (NGA/NASA) WGS 84 EGM96 Geopotential Model, hereafter refer to as EGM96. This product is a set of coefficients complete to degree and order 360, a companion set of correction coefficients needed to compute geoid height over land and a geoid height grid posted at 15 arc-minute spacing. On the other hand, heights measured relative to the geoid are called orthometric height (H) or, less formally, height above mean sea level. Orthometric heights are important, because these are the type of height found on innumerable topographic maps and in paper and digital datasets (see table 3.2). Using the above transformation parameter, the static GCP geoidal height information was computed using the UNAVCO calculator after adding the static GPS latitude, longitude and ellipsoidal height. A geoid height calculator is an online tool

that calculates the geoid height correction at a specified location on Earth using EGM96 gravity models.

In this study, there are three main phases involved which include the data acquisition (primary and secondary data), data processing and data analysis. These phases of research methodology are shown in (Fig 3.8).

Detailed have been made regarding system operations, data processing and workflow.

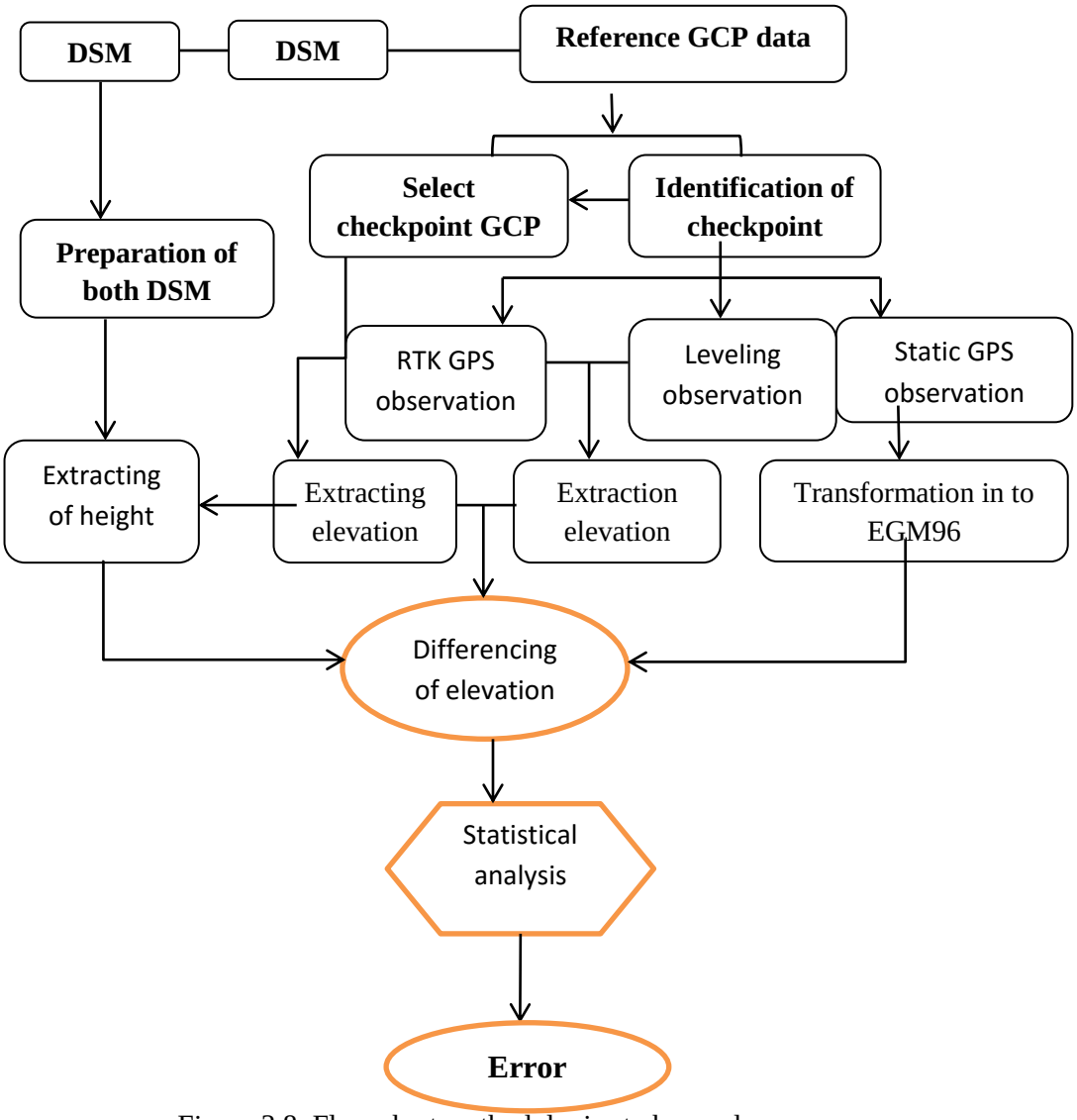

Figure 3.8: Flow chart methodologies to be used

3.4.2. Comparison of Checkpoint and GCP Elevation with Both DSM Elevation Data

The general principle of assessing the vertical accuracy of both DSM data sets was compared to the corresponding elevation point obtained from measured checkpoint and ground control points.

For calculating the accuracy of both DSM data, selected the urban land cover type specially, center of road in the study area. According to (ASPRS, 2004) the number of checkpoint selected from urban land cover type was 24 for GPS surveying and 10 for differential leveling. These points selected where, points are distributed sparsely across the project area and represents the full variety of the topography. In general, points were selected where points are identifiable on the free space and close to reference data exist in the study area. The difference between each checkpoint elevation which was used as reference and the corresponding elevation from both DSM data sets can be calculated by the following equation.

$$\Delta Z_I \quad = \quad Z_{data(i)} \; - \; Z_{check(j)} \qquad 3.4$$

Where $Z\_check(i)$ the elevation of the i^{th} measured checkpoint and GCP points which is used as a reference and $Z\_data(i)$ were the elevation from both DSM data would be tested at the i^{th} checkpoint.

The statistical parameters such as the range, absolute mean error and standard deviation or RMSE were calculated to get an accuracy assessment of the results. The accuracy of the fit is depicted by characterizing the distribution of error using the error population's estimated Root Mean Squired error.

In vertical accuracy assessments the NSSDA- specified and accepted measure of accuracy was the mean square root of squared differences between the DSM data and reference points. This term is called the root-mean-square error, or RMSE. RMSE is estimated from a sample of DSM data and reference points. The mean square root of the square of the differences was used to compensate for the fact that the errors can have both positive and negative values.

In this project, the acceptance of errors that used to evaluate the data was absolute mean, RMSE and 95% probabilities. The value of the data set can be calculated from

$$Absolute\ Mean \; = \; |\Delta Z| \quad = \quad \frac{\sum_{i=1}^{24} \left| \Delta Z data(i) \right|}{n} \qquad 3.5$$

$$RMSE \; = \; S \quad = \quad \pm \sqrt{\frac{\sum_{i=1}^{n} \left(\left(Zdata(i) - Zcheck(i) \right)^2 \right)}{n}} \qquad 3.6$$

These mathematical relation measures the difference between checkpoint elevation and both DSM elevation at a point which was derived from 2010 and 2016.

The estimate of the standard deviation (RMSE) of the squared differences was also an important parameter in many vertical accuracy assessment standards (Green walt and Schults, 1962, 1968; ASPRS, 1989). It also used to predict the range of standard normal distribution which the mean of population does exists based on the mean and standard deviation for a sample set. Any data set that observed in the study area contains three different types of errors: blunders or outliers, systematic and random. Carless observation or noise observation reading causes these error types. To avoid these types of errors especially blunders and systematic errors, induced by procedures or systematic and follow a fixed rule or specification standards (ASPRS, 2004). The basic idea of this rule was that if data follows a normal distribution and the data which has z-scores that exceeded 2(*RMSE*) in absolute value were considered as outliers. Higher percentage of errors used to help isolate outliers (very large errors) and blunders in the data set. Since outlier seldom occurs in the data set, measurements outside a selected high percentage range can be rejected as possible blunders. The elevation difference between both DSM elevation data and the three reference checkpoints followed a normal distribution the overall vertical accuracy at the 95 percent confidence level can be calculated (ASPRS, 2004). The NSSDA (FGDC, 1998) requires that accuracy be reported at the 95% level, which is defined by NSSDA as meaning "that 95% of the elevation in the data set would have an error with respect to true ground elevations that is equal to or smaller than the reported accuracy." NSSDA references the Greenwalt and Schultz (1962, 1968) equations, but *mistakenly* stipulates that the vertical accuracy interval at the 95% probability be computed by multiplying the appropriate *Zi* statistic (1.96) times the *estimated mean (*RMSE*)* instead of the *estimated standard deviation* (*S*). Note that the *Zi* (*S*) interval is not a confidence interval around the estimate of RMSE, nor was it has the range of expected errors at a given probability. It was an estimated of the maximum interval of error that existed at a specified probability assuming that mean error equals zero and the errors are normally distributed. The resulting NSSDA equation for calculating the NSSDA vertical accuracy statistic was;

$$NSSDA\ Vertical\ Accuracy\ =\ 1.96\ (RMSE) \qquad 3.7$$

The result that got from the difference between the checkpoint elevation and both DSM elevation data were tested using frequency histogram to see if they are normally distributed. To create a histogram the total data set were divided in to five classes. These were sub region of data that usually have a uniform range in values, or class width. As a rule of thumb, data sets of thirty values have only five or six classes. Using this rule of thumb, all the result of the data set of difference elevation was divided in to five classes and presented by frequency histogram.

CHAPTER FOUR

4. Results and Discussion

4.1 Results

4.1.1 Comparison between Static Deferential GPS Measurement and Existed GCP Point Elevation

Using LEICA_VIVA GS-14 receivers five static differential GPS measurement were performed at the point of existed GCP elevation point across the study area. The length of observation time at every bench mark is one hour interval. The sample of these points selected in a problematic way of the finding. The row data collected from the site was processed using differential approach with a tie to International GNSS service (IGS). This IGS data was used as a control which is adjusted and predicted the row data collected from field. The GPS elevation coordinate point values were then used as input in the geoid modeling software to determine the geoid heights for each point. These geoid heights were then subtracted from the GPS ellipsoidal heights to obtain orthometric height. Ellipsoidal heights (h), orthometric heights from spirit leveling (H level) and the orthometric height derived from the geoid modeling (H model) are the basic parameters used for evaluation of the geopotential model. Using the above transformation parameter, the selected static GCP geoidal height information's were computed using the UNAVCO calculator after adding the static GPS latitude, longitude and ellipsoidal height. The result of the row data was summarized (Table 4.1).

Table 4.1: Comparison between static measurement and existed GCP

No	GCP Name	Zcheck(i)	Zdata(i)	ΔZi	$(\mathbf{Zdata(i) - Zcheck(i)})^2$	A.Mean
1	KOREY MEKELAKEYA	2260.853	2261.9076	1.0546	1.11218116	1.0546
2	JEMO MEDHANILEM	2227.477	2228.5467	1.0697	1.14425809	1.0697
3	LAFTO MARUTA	2217.446	2218.5299	1.0839	1.17483921	1.0839
4	MIKAEL DILDIYE	2237.547	2238.5717	1.0247	1.05001009	1.0247
5	GEBRAEL DILDIYE	2222.032	2223.0474	1.0154	1.03103716	1.0154
	$\pm\sqrt{\frac{\sum_{i=1}^{5}\left((\mathbf{Zdata(i) - Zcheck(i)})^2\right)}{5}}$				$=\frac{5.512m}{5}$	
	$RMSE^2$				$=1.102m^2$	
	RMSE				= ±1.049m	
	A.MEAN				= 1.049m	

Source: Own Survey (2018)

The difference between the static elevation measurement and existed GCP elevation data set presented in the above (Table 4.1). The data value of the difference elevation of the five static measurement yields near to one. As listed in the above section 3, EGII stated that the maximum deviation of the vertical accuracy 18.1 centimeter was obtained. The elevation data value evaluated from above and the stated vertical accuracy of the associated Meta data of the existed GCP have a large difference. From the result, the height validation of five GCP elevation point gave a RMSE value of ±1.049 m and Absolute Mean value of 1.049 m. these implies that the accuracy of GCPs directly influences the accuracy of the final product. In this study the examined data derived from aerial photograph produced from these GCP points and also the reference checkpoint measurements' were performed using these GCP points. Finally, the examined elevation data and reference checkpoint elevation measurement affected by the initial error of the GCP elevation point and propagate or distribute the error by a rate of RMSE value of ±1.049 m elevation.

4.1.2. Comparison between GCP Elevation and DSM (2010) Elevation

Z elevation data vales collected from exited GCP, RTK GPS and differential leveling were compared with both DSM derived from aerial photograph. Sample data set below representing 24 GCP points were selected which are free from any disturbance and sparsely distributed across in the study area. Because the examined elevation data (DSM) are venerable by human made features (ASPRS, 2004). As explained in the introduction part DSM represents the surface of the earth includes all objects on it. They have direct relationship between GCP elevation and DSM derived from 2010 aerial photograph. Because, the exterior orientation of the image coordinate was rectified by using the existed GCP points. So the errors of the GCP propagate in the image coordinate. GCP elevation data was used as a reference for comparing the elevation extracting from DSM which is produced from 2010 aerial photograph by using GIS software package. After extracting the value of the point, absolute Mean, RMSE and 95% confidence level of probability were computed.

Analyzing the elevation accuracy involved using 24 GCP sample data to estimate the fit of DSM (2010) data being assessed to the reference point, which was assumed to correct. The accuracy of the fit was depicted by characterizing the distribution of error population estimated RMSE.

The statistical analysis for the entire process of height validation for the study area was summarized in Table 4.2. From this table's about 18 points of the data sets have negative value scored; meaning that the height level of GCP is lower than the examined data. Therefore, a clear negative bias for DSM was derived from 2010 aerial photograph on GCP checkpoint elevation. Using GCP elevation as a reference point, the vertical accuracy of DSM elevation data collected from 2010 gave a RMSE value of $\pm$0.68m and absolute mean value of $\pm$0.482m.

Table 4.2: Comparison between GCP elevation and DSM (2010) elevation**.**

No	GCP Name	Zcheck(i)	Zdata(i)	ΔZi	$(\mathbf{Zdata(i)} - \mathbf{Zcheck(i)})^2$	A.Mean
1	49	2235.991	2235.56	-0.430941	0.185	0.430941
2	151	2221.775	2221.58	-0.194922	0.037994586	0.194922
3	MKEN	2219.291	2218.612	-0.679	0.4610	0.679
4	4025	2249.477	2249.399	-0.077098	0.005944102	0.077098
5	CDCS	2268.809	2267.709	-1.099039	1.207886724	1.099
6	E136	2318.591	2318.84	0.249088	0.062044832	0.249
7	E178	2260.853	2260.37	-0.482883	0.233175992	0.48288
8	E180	2274.993	2275.36	0.367107	0.134767549	0.3671
9	E193	2240.138	2238.820	-1.317932	1.736944757	1.3179
10	E194	2226.458	2226.64	0.191902	0.036826378	0.1919
11	E208	2227.477	2227.30	-0.176951	0.031311656	0.17695
12	E211	2262.769	2262.89	0.130902	0.017135334	0.1309
13	E212	2228.617	2226.43	-2.177059	4.739585889	2.177059
14	E229	2254.122	2254.46	0.347971	0.121083817	0.34797
15	E233	2217.446	2217.370	-0.075883	0.00575823	0.07588
16	E247	2264.529	2264.449	-0.079049	0.006248744	0.079049
17	E249	2192.409	2191.620	-0.788883	0.622336388	0.788883
18	E260	2312.91	2312.590	-0.319912	0.102343688	0.319912
19	E265	2151.025	2150.560	-0.464941	0.216170133	0.46494
20	E273	2214.973	2214.639	-0.333107	0.110960273	0.333107
21	E288	2163.349	2162.409	-0.939088	0.881886272	0.939088
22	E359	2275.521	2275.209	-0.311039	0.09674526	0.311039
23	E361	2296.4	2296.310	-0.089941	0.008089383	0.089941
24	EZ63	2221.136	2221.370	0.234117	0.05481077	0.234117
			$\pm\sqrt{\frac{\sum_{i=1}^{24}\left((\mathbf{Zdata(i)}-\mathbf{Zcheck(i)})^2\right)}{24}}$		$=\frac{11.117\mathrm{m}}{24}$	
			$\boldsymbol{RMSE^2}$		$\mathbf{= 0.463}m^2$	
			RMSE		**= ±0.68m**	
			A.MEAN		**= ±0.482m**	
			RMSE(95%)		**= ±1.333m**	

Source: **(AACA, 2011**)

79.14% of the observation in a set of normally distributed total errors were lies between -0.68m and +0.68m (Table 4.2).These 79.14% observations were much greater than to the theoretical value of 68.3%. On the other hand, the standard error of 95% errors of the data set lies between $\pm$1.333m. This implies that, most of the data sets of the DSM (2010) precisely lie between $\pm$1.333m.

The data sets indicated that about 95.83% of the data set errors fall within the bounds of $\pm$1.333m standard error (Table 4.2). Implies that satisfied the error probability standard.

Table 4.3: Comparison between GCP and DSM (2010) elevation after removing outliers.

No	GCP Name	Z_check(i)	Z_data(i)	ΔZi	$(\mathbf{Z\_data(i) - Z\_check(i)})^2$	A.Mean(m)
1	49	2235.991	2235.56	-0.43094	0.18571	0.430941
2	151	2221.775	2221.58	-0.19492	0.037995	0.194922
3	4025	2249.477	2249.4	-0.0771	0.005944	0.077098
4	MKEN	2219.291	2218.612	-0.679	0.4610	0.679
5	E136	2318.591	2318.84	0.249088	0.062045	0.249
6	E178	2260.853	2260.37	-0.48288	0.233176	0.48288
7	E180	2274.993	2275.36	0.367107	0.134768	0.3671
8	E194	2226.458	2226.65	0.191902	0.036826	0.1919
9	E208	2227.477	2227.3	-0.17695	0.031312	0.17695
10	E211	2262.769	2262.9	0.130902	0.017135	0.1309
11	E229	2254.122	2254.47	0.347971	0.121084	0.34797
12	E233	2217.446	2217.37	-0.07588	0.005758	0.07588
13	E247	2264.529	2264.45	-0.07905	0.006249	0.079049
14	E249	2192.409	2191.62	-0.78888	0.622336	0.788883
15	E260	2312.91	2312.59	-0.31991	0.102344	0.319912
16	E265	2151.025	2150.56	-0.46494	0.21617	0.46494
17	E273	2214.973	2214.64	-0.33311	0.11096	0.333107
18	E288	2163.349	2162.41	-0.93909	0.881886	0.939088
19	E359	2275.521	2275.21	-0.31104	0.096745	0.311039
20	E361	2296.4	2296.31	-0.08994	0.008089	0.089941
21	EZ63	2221.136	2221.37	0.234117	0.054811	0.234117
$\pm\sqrt{\frac{\sum_{i=1}^{21}\left((\mathbf{Zdata(i) - Zcheck(i)})^2\right)}{21}}$					$= \frac{3.426\mathbf{m}}{21}$	
$\boldsymbol{RMSE^2}$					$\mathbf{= 0.172}\boldsymbol{m^2}$	
RMSE					**= ±0.415m**	
A.MEAN					**= ±0.332m**	

Source: **(AACA, 2011)**

According to the NSSDA specification, the data follows a normal distribution and the data which has z-scores that exceeded in absolute value were considered as outliers. So, we need to remove the outliers of the data set which, beyond from the bounds of 95% errors of probability (Table 4.3). The errors beyond to this bound were considered as systematic errors, because the selected GCP elevation points were affected by the surrounding objects.

After removing the outliers of the data set, the statistical analysis for the entire process of height validation for the study area is summarized (in Table 4.3). By using GCP height as a reference elevation, the absolute vertical accuracy of DSM elevation data collected from 2010 gave a RMSE value of ±0.415m and absolute mean value of ±0.332m. Means that, three data sets from the whole sample data have a value greater than 1.96X*RMSE* (±1.333m) were excluded from the statistical data. That means the examined data have surface elevation plus its surrounding objects at the selected GCP elevation point. In other way the data affected by systematic or gross error The data set tabulated in (Table 4.3) 71.43% of the observation in a set of normally distributed random errors lies between -0.415m and +0.415m. These 71.43% of the data set observations were much greater than that of the theoretical value of 68.3%. Finally, the accuracy DSM data achieved the national standard adopted by GII; DSM derived from aerial photograph was not exceeding three pixel size of ground sample distance (in z).

In order to represent the frequency distribution of the data sets we use a histogram bar graph. To create a histogram, the data set tabulated in Table 4.3 was divided in to five classes and subtracted the range from the largest to the smallest error value. Finally we got the class width of the interval. The range and the class width of the dataset tabulated in Table 4.3 was 1.306 and 0.2612 respectively. The first class interval is found by adding the class width to the lowest data value. For the data set in Table 4.3, the first class interval is from -0.678 to (-0.939 + 0.2612), or 0.678. This class interval includes all data from -0.939 up to, but not including, 0.680. Remaining class intervals are found by adding the class width to the upper boundary value of the preceding class. After creating class intervals, the number of data values in each interval is tallied. This is called the class frequency. Often, it is also useful to calculate the class relative frequency or number of occurrence for each interval. This is found by dividing the class frequency by the total number of observations. For the data set in Table 4.3, the class relative frequency for the first class interval is 3/21 = 0.143. The remaining class relative frequencies are

found by dividing the class frequency by the number of total observation. Notice that the sum of all class relative frequencies is always 1. The class relative frequency enables easy determination of percentages. For instance, the class interval from 0.131 to 0.367 contains 28.6% (0.286 × 100%) of the sample observations. It is the largest class relative frequency error depicted (Table 4.3).

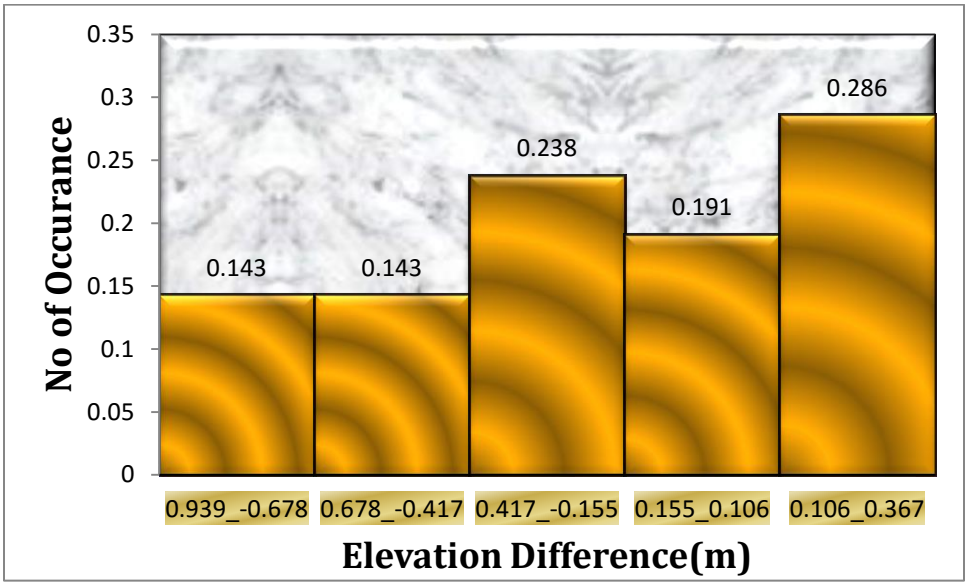

Figure 4.1: Elevation difference after deleting outliers (GCP-DSM (2010))

Using the data set of Table 4.3, the histogram shown in figure 4.1 was constructed. Notice that in this figure, class relative frequency or numbers of occurrence bounds on the ordinate, versus the class interval locate on the abscissa. Figure 4.1 represented bimodal and different distribution of the sample observation. It is histograms of elevation differences present a slightly negative skewer for examined data which indicates that the DSM data derived from 2010 aerial photograph underestimates the spatial distribution of terrain elevation. Therefore, there was a clear negative bias for DSM on GCP elevations. Finally, there is triple peak near to zero values and very narrow range with relatively shorter bar far from zero values to the left and larger bar graph far from zero values to the right (figure 4.1). The data set used to plotted in figure 4.1 were not précised and accurate than those used the data in figure 4.2.

4.1.3. Comparison between GCP Elevation and DSM (2016) Elevation

The data set below represents, 24 GCP points selected in randomly, where points are found in a problematic and sparsely distributed manner across the study area for the assessment of the data

DSM (2016). Similar to 2010 aerial photograph, the coordinate of the image depend on these GCP elevation points. So the elevation errors of the DSM have direct relation to that of the GCP elevation. Those GCP elevation points were the same reference point that of elevation selected for evaluated DSM (2010).

Table 4.4: Comparison between GCP elevation and DSM (2016) elevation.

No	GCP_name	Z_check(i)	Z_data(i)	ΔZi	$(\mathbf{Z\_data(i)} - \mathbf{Z\_check(i)})^2$	A.Mean(m)
1	49	2235.991	2236.376953	0.386	0.148996	0.386
2	151	2221.775	2222.011963	0.237	0.056169	0.237
3	E231	2233.38	2232.923096	-0.457	0.208849	0.457
4	4025	2249.477	2250.12793	0.651	0.423801	0.651
5	CDCS	2268.809	2268.981934	0.173	0.029929	0.173
6	E136	2318.591	2319.587891	0.997	0.994009	0.997
7	E178	2260.853	2261.096924	0.244	0.059536	0.244
8	E180	2274.993	2276.725098	1.732	2.999824	1.732
9	E193	2240.138	2240.406982	0.269	0.072361	0.269
10	E194	2226.458	2226.968018	0.51	0.2601	0.51
11	E208	2227.477	2227.846924	0.369	0.136161	0.369
12	E211	2262.769	2263.282959	0.514	0.264196	0.514
13	E212	2228.617	2229.291992	0.675	0.455625	0.675
14	E229	2254.122	2254.36792	0.246	0.060516	0.246
15	E233	2217.446	2217.481934	0.036	0.001296	0.036
16	E247	2264.529	2264.802002	0.273	0.074529	0.273
17	E249	2192.409	2194.064941	1.656	2.742336	1.656
18	E260	2312.91	2313.022949	0.113	0.012769	0.113
19	MKEN	2219.291	2219.97	0.679	0.461041	0.679
20	E273	2214.973	2216.042969	1.07	1.1449	1.07
21	E288	2163.349	2163.193115	-0.156	0.024336	0.156
22	E359	2275.521	2276.50708	0.986	0.972196	0.986
23	E361	2296.4	2298.224121	1.824	3.326976	1.824
24	EZ63	2221.136	2221.051025	-0.085	0.007225	0.085
$\pm\sqrt{\frac{\sum_{i=1}^{24}\left((\mathbf{Zdata(i)}-\mathbf{Zcheck(i)})^2\right)}{24}}$				$=\frac{14.938\mathbf{m}}{24}$		
$\boldsymbol{RMSE^2}$				$= 0.622\boldsymbol{m^2}$		
RMSE				$= \pm 0.789$M		
A.MEAN				$= \pm 0.597$m		
RMSE(95%)				$= \pm 1.546$m		

Source: **(AACA, 2011**)

The statistical analysis for the entire process of height validation for the study area is summarized in the above Table 4.4. As it can be deduced from the above table about 3 points of observations have negative values meaning that most of the height level of GCP is lower than the examined data. This data set implies that the DSM (2016) upper estimates the spatial distribution of terrain elevation. By using GCP height as a reference elevation the vertical accuracy of DSM elevation data derived from 2016 gave a RMSE and absolute mean value of ±0.789m and ±0.597m respectively (table 4.4). 79.166% of the observations in a set of normally distributed random errors lies between -0.789m and +0.789m. About 79.166% observations were greater than to that of the theoretical value of 68.3%. On the other hand, the RMSE of 95% probability level errors of the data set value that was summarized from Table 4.4 lies between ±1.546m. It was an estimated of the maximum interval of error that existed at a specified probability assuming that mean error equals zero and the errors are normally distributed. From this data set, four data sets have greater than the probability confidence interval of ±1.546 means that, beyond to the confidence interval removed from the data sets. Because those of the data set errors induced by systematic or blunder errors. About 83.333% of the data set errors failed within the bounds of ±1.546m probability error of the total population (Table 4.4).

Table 4.5: Comparison between GCP and DSM (2016) elevation after removing outliers.

No	GCP _Name	Z_check(i)	Z_data(i)	ΔZi	$(\mathbf{Z\_data(i) - Z\_check(i)})^2$	A.Mean(m)
1	49	2235.991	2236.376953	0.386	0.148996	0.386
2	151	2221.775	2222.011963	0.237	0.056169	0.237
3	4025	2249.477	2250.12793	0.651	0.423801	0.651
4	CDCS	2268.809	2268.981934	0.173	0.029929	0.173
5	E136	2318.591	2319.587891	0.997	0.994009	0.997
6	E178	2260.853	2261.096924	0.244	0.059536	0.244
7	E193	2240.138	2240.406982	0.269	0.072361	0.269
8	E194	2226.458	2226.968018	0.51	0.2601	0.51
9	E208	2227.477	2227.846924	0.369	0.136161	0.369
10	E211	2262.769	2263.282959	0.514	0.264196	0.514
11	E212	2228.617	2229.291992	0.675	0.455625	0.675
12	E229	2254.122	2254.36792	0.246	0.060516	0.246
13	E231	2233.38	2232.923096	-0.457	0.208849	0.457
14	E233	2217.446	2217.481934	0.036	0.001296	0.036
15	E247	2264.529	2264.802002	0.273	0.074529	0.273
16	E260	2312.91	2313.022949	0.113	0.012769	0.113
17	MKEN	2219.291	2219.97	0.679	0.461041	0.679
18	E288	2163.349	2163.193115	-0.156	0.024336	0.156
19	E359	2275.521	2276.50708	0.986	0.972196	0.986
20	E263	2221.136	2221.051025	-0.085	0.007225	0.085
$\pm\sqrt{\frac{\sum_{i=1}^{20}\left((\mathbf{Zdata(i)-Zcheck(i)})^2\right)}{20}} = \frac{4.724\mathbf{m}}{20}$						
$\boldsymbol{RMSE^2}$					$\mathbf{=0.236}\boldsymbol{m^2}$	
RMSE					**= ±0.486m**	
A.MEAN					**=±0.403m**	

Source: **(AACA, 2011**)

After removing the outliers of the data set, the statistical computation for the entire process of height validation for the study area was summarized (in Table 4.5). By using GCP height as a reference elevation the absolute vertical accuracy of DSM elevation data derived from 2016 gave a RMSE value of $\pm$0.486m and absolute mean value of $\pm$0.403m (Table 4.5). These values were less accurate than that of data compared DSM (2010). As stated in the introduction, the accuracy of DSM data was influenced by the flight altitude, resolution of the data and so on. Due to these reason the data derived from 2016 aerial photograph have low resolution and high flight altitude than the data derived from 2010 aerial photograph. Four data sets from the whole sample data

have a value greater than 1.96X*RMSE* (±1.546m) excluded (Table 4.5). 65% of the observation in a set of normally distributed random errors lies between -0.486m and +0.486m (Table 4.5). These 65% of the data set observations were much closer to the theoretical value of 68.3%. Finally, the accuracy assessment of DSM (2016) data also achieved the national standard adopted by EGII.

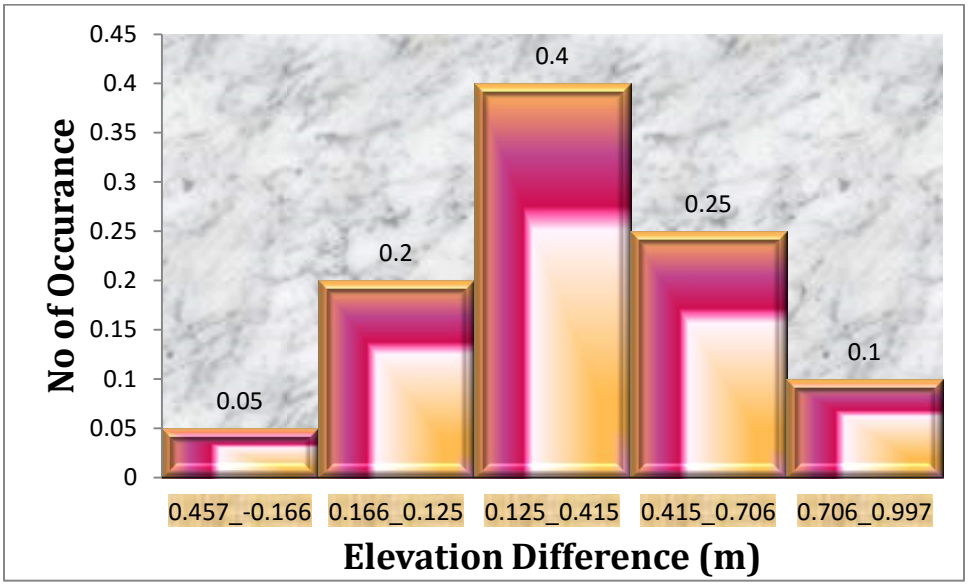

Figure 4.2: Elevation difference after removing outliers (GCP-DSM (2016))

Table 4.3 and Table 4.5 represents the frequency distribution by using a histogram bar graph. In order to represent the data set of table 4.5 we use the step of calculating range and class width of figure 4.1. So, the range and the class width of the dataset tabulated in Table 4.5 was 1.45 and 0.29 respectively. The class interval from 0.173 to 0.386 contains 40% (0.40 × 100%) of the sample observations. It is the largest class relative frequency error depicted in Figure 4.2. The errors of the both DSM data were evaluated by using the same GCP reference. Comparatively, figure 4.2 have shorter bar graph near to zero values and lower range than that of Figure 4.1. In the above histogram, there is a single peak to the right of zero value. So, DSM (2016) relatively have high precise but less accurate data set yield as compared to the data set of DSM (2010). But, Figure 4.2 represented the histograms of elevation differences have symmetrical and normal distribution from the center value than that of depicted Figure 4.1 and the shape of the figure looks like a bell curve. It would mean that the frequencies were equally distributed. From this figure the pick point represent the middle which is the highest value group of the data. The

distribution of histogram present in Figure 4.2 have slightly positive skewness for examined data which indicated that the DSM data derived from 2016 aerial photograph overestimates the spatial distribution of terrain elevation. Therefore, there was a clear positive bias for DSM on GCP elevations.

4.1.4. Comparison between GPS Checkpoint Elevation and DSM (2010) Elevation

As indicated in Table 4.6, 24 GPS checkpoint elevations were selected randomly, where points were found in free from any disturbance and sparsely distributed manner across the study area, for the assessment of DSM data which derived from 2010 aerial photograph.

The statistical computation for the entire process of height validation for the study area is summarized in the above table, Table 4.6. From these tables about 15 points of the deductive have negative values, inferring that the point of height level of the checkpoint is higher than that of the examined data which indicates the data under estimate of the spatial distribution of the terrain elevation. This implies that the data derived from 2010 aerial photograph underestimates the spatial distribution than that of derived from 2016 aerial photograph. These values are significantly similar to the data's summarized in table 4.2. On the other hand, 9 points of observation for the study area have positive value, indicating that the height level of the GPS checkpoint elevation is lower than the examined data Therefore, a clear negative bias for DSM is derived from 2010 aerial photograph on GPS checkpoint elevation. According to the NSSDA specification, the data follows a normal distribution and the data which has z-scores that exceeded in absolute value were considered as systematic error or outliers.

Table 4.6: Comparison between GPS checkpoint and DSM (2010) elevation

No	Site_ Name	Z_check(i)	Z_data(i)	ΔZi(m)	$(\mathbf{Z\_data(i)} - \mathbf{Z\_check(i)})^2$	A.Mean (m)
1	Kotari 66	2232.226	2231.04	-1.185961	1.406503494	1.186
2	Kotari 65	2247.654	2243.99	-3.66401	13.42493264	3.66401
3	Mamo 78	2285.889	2285.6799	-0.209068	0.043709429	0.209
4	Mamo 77	2281.38	2281.98	0.59998	0.359976	0.599
5	Hanatebel 69	2156.051	2153.8799	-2.171117	4.713749028	2.171
6	Hanatebel 68	2204.48	2203.3799	-1.100117	1.210257414	1.1
7	Hanatebel 67	2184.596	2184.6899	0.093941	0.008824911	0.094
8	B.Gebrael 81	2318.356	2318.23	-0.126	0.015876	0.126
9	B.Gebrael 80	2301.845	2302.02	0.175	0.030625	0.175
10	B.Gebrael 79	2269.188	2268.79	-0.397961	0.158372958	0.398
11	Gofa 42	2272.479	2270.21	-2.269	5.148	2.269
12	Gurage D29	2225.791	2225.8501	0.059098	0.003492574	0.059
13	Gurage D28	2217.603	2218.03	0.427029	0.182353767	0.427
14	Gurage D27	2241.349	2240.8601	-0.488893	0.239016365	0.239
15	Maruta 574	2218.363	2217.28	-1.082971	1.172826187	1.083
16	Maruta 573	2258.599	2257.55	-1.049	1.100401	1.049
17	Maruta 571	2214.665	2214.1899	-0.4751	0.22572	0.4751
18	Maruta 572	2214.899	2215.22	0.321	0.103	0.321
19	Jemo 51	2229.318	2229.49	0.17199	0.02958056	0.172
20	Jemo 50	2237.214	2236.6201	-0.593883	0.352697018	0.594
21	Jemo 49	2238.857	2238.72	-0.137029	0.018776947	0.137
22	Jemo 48	2235.296	2235.5601	0.264059	0.069727155	0.264
23	Jemo 46	2228.058	2227.3	-0.757951	0.574489718	0.758
24	Jemo 47	2231.817	2232.0601	0.243059	0.059077677	0.243
$\pm\sqrt{\frac{\sum_{i=1}^{24}\left((\mathbf{Zdata(i)}-\mathbf{Zcheck(i)})^2\right)}{24}} = \frac{30.652\mathbf{m}}{24}$						
$\boldsymbol{RMSE^2}$				$\mathbf{= 1.277}\boldsymbol{m^2}$		
RMSE				**= ±1.13m**		
A.MEAN				**= ± 0.727m**		
RMSE(95%)				**=±2.215m**		

Source: Own Survey (2018)

By using checkpoint height as a reference elevation the vertical accuracy of DSM elevation data derived from 2010 gave the RMSE value of ±1.13m and Absolute Mean value of ±0.727m (Table 4.6). From this data set, three data sets have greater than *1.96xRMSE* were an outliers. Because, the checkpoint elevation were measured where the point were far from the reference

GCP point or the examined data may be affected by surrounding objects. 83.333% of the observations in a set of normally distributed random errors lie between -1.13m and +1.13m. These 83.333% observations were greater than the theoretical value of 68.3%. On the other hand, the probability standard error of 95% errors of the data set lies between $\pm$2.215m. From the above data sets indicates that, about 87.5% of the data set errors fall within the bounds of $\pm$2.215m standard error (Table 4.6). It is the confidence interval of the total population. Finally, the data set value that exceeds from 95% probability errors were considered as outliers or gross error. So, these data sets are removed from the above analyzed data set (Table 4.7).

Table 4.7: Comparison between GPS checkpoint and DSM (2010) elevation after removing outliers.

No	Site _Name	Z_check(i)	Z_data(i)	ΔZi(m)	$(\mathbf{Z\_data(i) - Z\_check(i)})^2$	A.Mean(m)
1	Kotari 66	2232.2	2231.04	-1.18596	1.406503	1.186
2	Mamo 78	2285.9	2285.68	-0.20907	0.043709	0.209
3	Mamo 77	2281.4	2281.98	0.59998	0.359976	0.599
4	Hanatebel 68	2204.5	2203.38	-1.10012	1.210257	1.1
5	Hanatebel 67	2184.6	2184.69	0.093941	0.008825	0.094
6	B.Gebrael 81	2318.4	2318.23	-0.126	0.015876	0.126
7	B.Gebrael 80	2301.8	2302.02	0.175	0.030625	0.175
8	B.Gebrael 79	2269.2	2268.79	-0.39796	0.158373	0.398
9	Gurage D29	2225.8	2225.85	0.059098	0.003493	0.059
10	Gurage D28	2217.6	2218.03	0.427029	0.182354	0.427
11	Gurage D27	2241.3	2240.86	-0.48889	0.239016	0.239
12	Maruta 574	2218.4	2217.28	-1.08297	1.172826	1.173
13	Maruta 573	2258.6	2257.55	-1.049	1.100401	1.049
14	Maruta 571	2214.7	2214.19	-0.4751	0.22572	0.4751
15	Maruta 572	2214.9	2215.22	0.321	0.103	0.321
16	Jemo 51	2229.318	2229.49	0.17199	0.029581	0.172
17	Jemo 50	2237.214	2236.62	-0.59388	0.352697	0.594
18	Jemo 49	2238.857	2238.72	-0.13703	0.018777	0.137
19	Jemo 48	2235.296	2235.56	0.264059	0.069727	0.264
20	Jemo 46	2228.058	2227.3	-0.75795	0.57449	0.758
21	Jemo 47	2231.817	2232.06	0.243059	0.059078	0.243
$\pm\sqrt{\frac{\sum_{i=1}^{21}\left((\mathbf{Zdata(i)-Zcheck(i)})^2\right)}{21}} = \frac{7.365\mathbf{m}}{21}$						
$\boldsymbol{RMSE^2}$				$\mathbf{=0.35}m^2$		
RMSE				**= ±0.592m**		
A.MEAN				**= ± 0.466m**		

After removing the outliers of the data sets, the statistical computation for the entire process of height validation for the study area were summarized in Table 4.7. By using GPS checkpoint height as a reference elevation the vertical accuracy of DSM elevation data derived from 2010 gave a RMSE value of ±0.592m and Absolute Mean value of ±0.35m (Table 4.7). The value indicates that they have slightly greater than that of a data examined by GCP height reference. Suggesting that three data sets from the whole sample data have a value greater than 1.96X*RMSE* (±2.215m) excluded. Finally, the RMSE error value of the data set based on RTK GPS achieves the national standard specification adopted the EGII.

The data set represented in Table 4.7 also analyzed by using histogram bar. The same to like the above histogram representation, the data set plotted with relative class frequency on the ordinate, versus error values of the class interval bounds on the abscissa. The difference is that represented in table 4.7 from table 4.3 and table 4.5 were reference of data observation. The data set depicted in figure 4.3 was measured the points by RTK GPS with reference from GCP point.

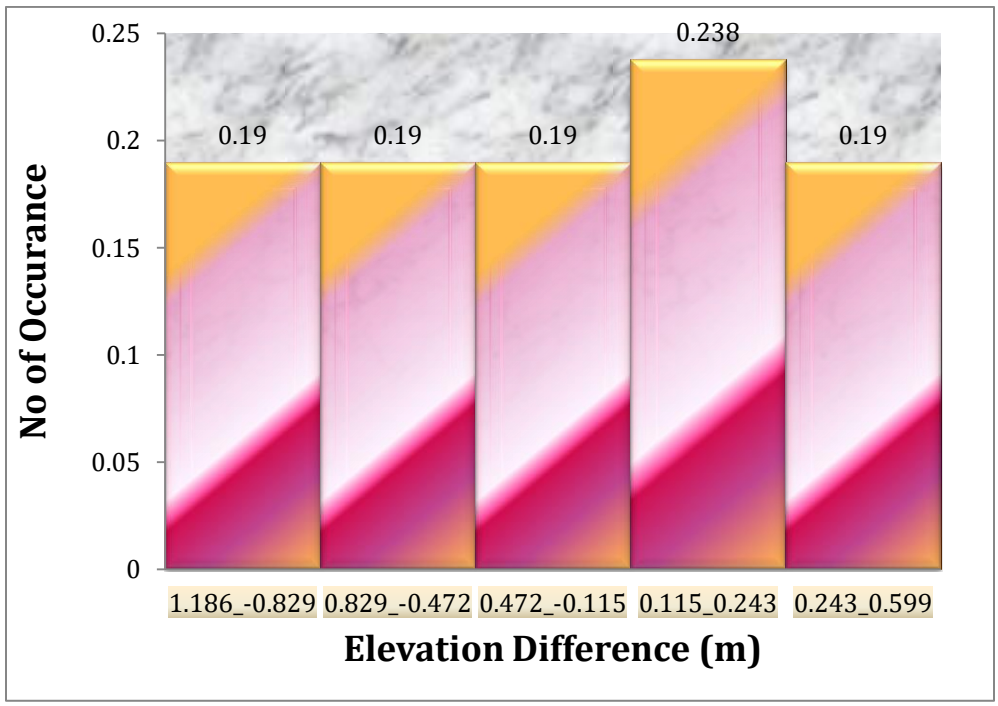

Figure 4.3: Elevation difference after removing outliers (RTK GPS- DSM (2010))

The range and the class width of the dataset tabulated in Table 4.7 was 1.785 and 0.357 respectively. It is an indication of the precision of the data set. The range for this data set can be compared with the range of both data sets that is table 4.3 and table 4.5 was slightly higher. For

instance, the class interval from -0.115 to 0.243 contains 23.8% (0.238 × 100%) of the sample observations. It is the largest class relative frequency error depicted in table 4.7. Figure 4.3 represented skewed and asymmetrical shape distribution to the right. Like figure 4.1 it have a slightly negative skewness for examined data which indicates that the DSM data derived from 2010 aerial photograph underestimates the spatial distribution of terrain elevation. Therefore, there was a clear negative bias for DSM on GPS elevations. Finally, in the histogram of Figure 4.3, there is single peak near to zero values and larger range with relatively to the dataset tabulated in Table 4.2. But, it hasn't a normal distribution unlike, the data set depicted in Figure 4.2 and it has less accurate and precise data error in the table.

4.1.5. Comparison between GPS Checkpoint Elevation and DSM (2016) Elevation

The data set below represents, 24 GPS checkpoint elevations observed randomly, where points were free from GPS errors and sparsely distributed across the study area for the assessment of the data DSM (2016). These data were collected where points are close to the reference elevation and free from error that disturbs leveling measurements.

The statistical examination for the entire process of height validation for the study area is summarized in Table 4.8. From these tables about five points of observations have negative value suggesting that the height level of GPS checkpoint elevation is lower than the examined data. By using GPS observation as a reference elevation the vertical accuracy of DSM elevation data derived from 2016 aerial photographs gave a RMSE and Absolute Mean values of $\pm$1.173m and $\pm$0.899m respectively (table 4.8). These data sets imply that 70.833% of the observations in a set of normally distributed random errors have lied between -1.173m and +1.173m. These 70.833% observations are very close to the theoretical value of 68.3%. According to the NSSDA specification, the data follows a normal distribution and the data which has z-scores that exceeded in absolute value were considered as outliers. From this data set, three data sets have greater than 1.96XRMSE meanings that, about 83.333% of all observations were retained in the specification, similar to that of the data 2010 aerial photograph. On the other hand, the standard error of 95% probability errors of the data set lies between $\pm$2.299. Indicates that the total error of the population of the target area. The number of data sets in Table 4.8 indicated that about 17% of the data sets were affected by the various types and potential source of interference of the observation and the examined data. Beyond this data set bounds considered as a blunders. Then

we need to exclude the systematic and gross error greater than 1.96XRMSE error probability (See Table 4.9).

Table 4.8: Comparison between checkpoint and DSM (2016) elevation.

No	Point_name	Z_check(i)	Z_data(i)	ΔZi	$(Z\_data(i) - Z\_check(i))^2$	A.Mean(m)
1	Kotari 66	2232.226	2230.821	-1.40496	1.97389855	1.404955
2	Kotari 65	2247.654	2245.215	-2.4386	5.94676996	2.4386
3	Mamo 78	2285.889	2288.364	2.475014	6.1256943	2.475014
4	Mamo 77	2281.38	2281.803	0.422979	0.17891123	0.422979
5	Hanatebel 69	2156.051	2154.861	-1.18992	1.41590009	1.189916
6	Hanatebel 68	2204.48	2204.828	0.347881	0.12102119	0.347881
7	Hanatebel 67	2184.596	2184.78	0.184029	0.03386667	0.184029
8	B.Gebrael 81	2318.356	2318.453	0.096881	0.00938593	0.096881
9	B.Gebrael 80	2301.845	2302.182	0.336885	0.1134915	0.336885
10	B.Gebrael 79	2269.188	2267.983	-1.20509	1.45224191	1.20509
11	Gofa 42	2272.479	2275.295	2.815922	7.92941671	2.815922
12	Gurage D29	2225.911	2226.109	0.197887	0.03915926	0.197887
13	Gurage D28	2217.603	2218.183	0.580105	0.33652181	0.580105
14	Gurage D27	2241.349	2241.905	0.556029	0.30916825	0.556029
15	Maruta 574	2218.363	2219.03	0.667029	0.44492769	0.667029
16	Maruta 573	2258.599	2259.758	1.159012	1.34330882	1.159012
17	Maruta 571	2214.665	2215.246	0.5806	0.33709636	0.5806
18	Maruta 572	2214.899	2215.244	0.344896	0.11895325	0.344896
19	Jemo 51	2229..318	2230.11	0.792	0.627264	0.792
20	Jemo 50	2237.214	2238.19	0.975941	0.95246084	0.975941
21	Jemo 49	2238.857	2239.256	0.399	0.159201	0.399
22	Jemo 48	2235.81	2237.456	1.646055	2.70949706	1.646055
23	Jemo 46	2228.058	2227.84	-0.21799	0.04752016	0.217991
24	Jemo 47	2231.817	2232.363	0.546037	0.29815641	0.546037
$\pm\sqrt{\frac{\sum_{i=1}^{24}\left((Zdata(i)-Zcheck(i))^2\right)}{24}} = \frac{33.024m}{24}$						
$RMSE^2$			= $1.376m^2$			
RMSE			= ±1.173m			
A.MEAN			= ±0.899			
RMSE(95%)			=± 2.299m			

Source: Own Survey (2018)

After removing the outliers of the data set, the statistical computation for the entire process of height validation for the study area was summarized in Table 4.9. By using observation checkpoint height as a reference the vertical accuracy of DSM elevation data derived from 2016 gave a RMSE and Absolute Mean value of $\pm$0.787m and $\pm$0.659m respectively (Table 4.9). This implies that the value was significantly larger error than that of the examined DSM data derived from 2010 aerial photograph.

Table 4.9: Comparison between GPS checkpoint and DSM (2016) elevation after removing outliers.

No	Point_Name	Z_check(i)	Z_data(i)	ΔZi	$(\mathbf{Z\_data(i)} - \mathbf{Z\_check(i)})^2$	A.Mean(m)
1	Kotari 66	2232.226	**2230.821**	**-1.40496**	**1.973899**	**1.404955**
2	Mamo 77	2281.38	2281.803	0.422979	0.178911	0.422979
3	Hanatebel 69	2156.051	2154.861	-1.18992	1.4159	1.189916
4	Hanatebel 68	2204.48	2204.828	0.347881	0.121021	0.347881
5	Hanatebel 67	2184.596	2184.78	0.184029	0.033867	0.184029
6	B.Gebrael 81	2318.356	2318.453	0.096881	0.009386	0.096881
7	B.Gebrael 80	2301.845	2302.182	0.336885	0.113492	0.336885
8	B.Gebrael 79	2269.188	2267.983	-1.20509	1.452242	1.20509
9	Gurage D29	2225.911	2226.109	0.197887	0.039159	0.197887
10	Gurage D28	2217.603	2218.183	0.580105	0.336522	0.580105
11	Gurage D27	2241.349	2241.905	0.556029	0.309168	0.556029
12	Maruta 574	2218.363	2219.03	0.667029	0.444928	0.667029
13	Maruta 573	2258.599	2259.758	1.159012	1.343309	1.159012
14	Maruta 571	2214.665	2215.246	0.5806	0.337096	0.5806
15	Maruta 572	2214.899	2215.244	0.344896	0.118953	0.344896
16	Jemo 51	2229..318	2230.11	0.792	0.627264	0.792
17	Jemo 50	2237.214	2238.19	0.975941	0.952461	0.975941
18	Jemo 49	2238.857	2239.256	0.399	0.159201	0.399
19	Jemo 48	2235.81	2237.456	1.646055	2.709497	1.646055
20	Jemo 46	2228.058	2227.84	-0.21799	0.04752	0.217991
21	Jemo 47	2231.817	2232.363	0.546037	0.298156	0.546037
$\pm\sqrt{\frac{\sum_{i=1}^{21}\left((\mathbf{Zdata(i)}-\mathbf{Zcheck(i)})^2\right)}{21}} = \frac{\mathbf{13.022m}}{21}$						
$\boldsymbol{RMSE^2}$				$= 0.62\boldsymbol{m^2}$		
RMSE				$= \pm 0.787$m		
A.MEAN				$= \pm 0.659$m		

71.42% of the observations in a set of normally distributed random errors lies between -0.787m and +0.787 (Table 4.9). These 71.42% of the data set observations were greater than that of the theoretical value which is 68.3%.

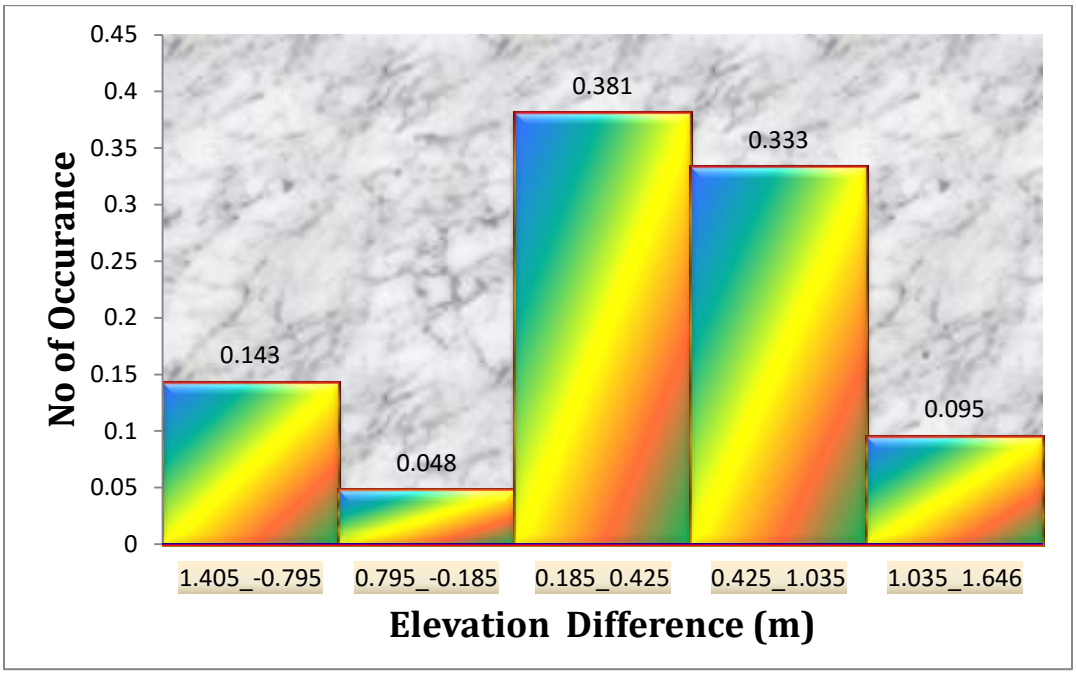

Figure 4.4: Elevation difference after removing outliers (RTK GPS- DSM (2016)).

Like the data set tabulated in table 4.7, the data set depicted in figure 4.4 was measured the checkpoints by RTK GPS with reference from GCP point. The difference was the time and method of existed DSM data observation of the aerial photograph. By using the analyzed tool, the range and the class width of the dataset tabulated in Table 4.9 was 3.051 and 0.61 respectively. It also an indication of the precision of the data set as compared to the other data set. The range and class width for this data set can be compared with the range of those data sets that is table 4.3, table 4.5 and table 4.7 was slightly higher. For instance, the class interval from -0.185 to 0.425 contains 38.10% (0.381 × 100%) of the sample observations. That is, the larger percentage of the sample observation lies near to right and left of zero value. It is the largest class relative frequency error depicted near to zero values. Figure 4.1 and Fig 4.4 represented a normal distribution and symmetrical shape of the central zero value. But it has less accurate than the data presented in figure 4.2 and it has high precision of the data presented in (Fig 4.1 and Fig 4.3).

4.1.6. Comparison between Differential Leveling and DSM (2010) Elevation

Another method of assessing the accuracy of both examined data's was differential leveling. For analyzing these examined data ten sampling data was selected and observed in the study area. As indicated from below, the statistical analysis for the entire process of height validation for the study area is summarized in Table 4.10.

Table 4.10: Comparison between leveling and DSM (2010) elevation.

NO	Site_Name	X	Y	Z_check(i)	Z_data(i)	ΔZi(m)	$(\text{Z\_data(i)} - \text{Z\_check(i)})^2$	A.Mean(m)
1	Jemo(46)	468503.353	989612.33	2227.32	2227.3	-0.02	0.0004	0.02
2	Jemo(47)	468749.834	989384.6	2232.24	2232.06	-0.18	0.033	0.18
3	Jemo(48)	468200.514	990263.13	2235.81	2235.56	-0.25	0.063	0.25
4	Jemo(51)	469566.596	989017.26	2230.66	2229.49	-1.167	1.361889	1.167
5	Gurage.D(27)	469220.876	991311.19	2239.99	2240.86	-0.13	0.017	0.13
6	Gurage.D(28)	470578.07	990759.79	2216.73	2218.03	1.296	1.679616	1.296
7	Gurage.D(29)	470421.23	991730.47	2225.456	2224.64	-0.816	0.666	0.816
8	Hana Tebel(67)	472336.706	988013.4	2184.02	2184.69	0.666	0.443556	0.666
9	Hana Tebel(69)	473021.456	986999.79	2153.93	2153.88	-0.052	0.002704	0.052
10	Mamo(77)	473899.563	991661.36	2281.38	2281.98	0.599	0.358801	0.599
$\pm\sqrt{\frac{\sum_{i=1}^{10}\left((\text{Zdata(i)}-\text{Zcheck(i)})^2\right)}{10}}=\frac{4.626\text{m}}{10}$								
$RMSE^2$					$=0.463m^2$			
RMSE					= ±0.68m			
A.MEAN					= ±0.518m			
RMSE(95%)					= ±1.334m			

From these tables about seven points of observations have negative value means that the height level of checkpoint is lower than the examined data. By using a method of differential leveling as a reference elevation the vertical accuracy of DSM elevation data derived from 2010 aerial photographs gave RMSE and absolute mean value of $\pm$0.68m and $\pm$0.518m respectively (Table 4.10). From this data set, no data set has greater than 1.96xRMSE means that, about 100% of all observations were retained in the specification. These data sets imply that 70% of the observations in a set of normally distributed random errors have lies between -0.68m and +0.68m. These 70% observations are very close to the theoretical value of 68.3%. On the other

hand, the standard error of 95% probability errors of the data set lies between ±1.334m. The number of data sets in Table 4.10 indicated that about 100% of the data set errors fall within the bounds of ±1.334m standard error. Beyond to this data set bounds considered as a blunders.

4.1.7. Comparison between Differential Leveling and DSM (2016) Elevation

Another checkpoint data that examined using this differential leveling was DSM derived from aerial photograph (2016). Similar to the above Table 4.10, ten sampling data were selected in the study area at the same point where RTK GPS measurement was taken. As indicated from below, the statistical analysis for the entire process of height validation for the study area is summarized in Table 4.11. From these tables one point of observation has negative value.

Table 4.11: comparison between leveling and DSM (2016) elevation

NO	Site_Name	X	Y	Z_check(i)	Z_data(i)	ΔZi(m)	$(\text{Z\_data(i)} - \text{Z\_check(i)})^2$	A.Mean(m)
1	Jemo(46)	468503.4	989612.3	2227.32	2227.840088	0.520088	0.270492	0.520088
2	Jemo(47)	468749.8	989384.6	2232.24	2232.363037	0.123037	0.015138	0.123037
3	Jemo(48)	468200.5	990263.1	2235.81	2237.456055	1.646055	2.709497	1.646055
4	Jemo(51)	469566.6	989017.3	2230.66	2230.110107	-0.54989	0.302382	-0.54989
5	Gurage.D(27)	469220.9	991311.2	2240.99	2241.905029	0.915	0.837	1.915029
6	Gurage.D(28)	470578.1	990759.8	2216.73	2218.183105	1.453105	2.111514	1.453105
7	Gurage.D(29)	470421.2	991730.9	2225.456	2226.108887	0.652887	0.426261	0.652887
8	Hana Tebel(67)	472336.7	988013.4	2184.02	2184.780029	0.760029	0.577644	0.760029
9	Hana Tebel(69)	473021.5	986999.8	2153.93	2154.861084	0.931084	0.866917	0.931084
10	Mamo(77)	473899.6	991661.4	2281.38	2281.802979	0.422979	0.178911	0.422979
					$\pm\sqrt{\frac{\sum_{i=1}^{10}\left((\text{Zdata(i)}-\text{Zcheck(i)})^2\right)}{10}}$		$=\frac{8.296\text{m}}{10}$	
					$RMSE^2$		$=0.83m^2$	
					RMSE		= ±0.911m	
					A.MEAN		=±0.897m	
					RMSE(95%)		=±1.786m	

Using a method of differential leveling as a reference elevation, the vertical accuracy of DSM elevation data derived from 2016 Aerial Photographs gave RMSE and absolute mean value of ±0.911m and ±0.897m respectively (Table 4.11). From this data set, no data set has greater than 1.96XRMSE means that, about 100% of all observations were retained in the specification.

These data sets imply that 70% of the observations in a set of normally distributed random errors have lies between -0.911m and +0.911m. These 70% observations are very close to the theoretical value of 68.3%. On the other hand, the standard error of 95% probability errors of the data set lies between ±1.786m. About 100% of the data set errors fall within the bounds of ±1.786m standard error.

4.2. Discussion

In this study, two DSM data collected from INSA which were acquired in the period of 2010 and 2016 G.C were investigated using three reference elevation data. These reference checkpoint elevations was depends on the existed GCP point across the study area. In order to increase the acceptance of the data evaluated by the check point, five static GPS measurement method was performed independently for a length of one hour interval. The validation result of the five GCP elevation measurements gave a RMSE value of ±1.049 m and Absolute Mean value of 1.049 m. These result were strictly different that the error of the GCP elevation specified by EGII. As we stated in the introduction section the accuracy level of GCP point was affected the final product of DSM derived from aerial photograph. Checkpoint elevations were selected randomly, free from any disturbance, sparsely distributed across the area and their problematic in major urban land use type. Because, they are used to minimize the disturbance of the measurement's and covered the total population of the study area. Points that are observed from the field which have large error value in the data set may be affected by the distance between the GCP reference and the checkpoint to be measured and the surrounding building that diverts the receiving incoming signals. And also sizes of the sample point have different error value we got from the examined data. Before performing statistical computation, the blunders and systematic errors were removed using the formula of 1.96xRMSE. It gives an overall accuracy assessment at 95 percent of confidence level of the total study area. Based on the result obtained from in this study, the statistical computation for DSM (2010) and DSM (2016) vertical accuracy elevation data in the study area gave a RMSE value of ±0.415m and ±0.486m and absolute mean value of ±0.332m and ±0.403m, respectively where GCP were used as an independent reference point. They have similar result that reported in the previous studies obtained in a RMSE error of 0.41 and absolute mean value of 0.48 with a large scale of 1:5000 aerial photograph generation (Lella et al., 2012). Where RTK GPS leveling measurement was performed as a reference in the study area, the

statistical value of the point indicated the vertical accuracy of DSM (2010) and DSM (2016) data was gave us a RMSE error of ±0.592m and ±0.787m, absolute mean error value of ±0.466m and ±0.659m, respectively. This result was slightly similar to the previous study reported a RMSE value of 0.55m with a scale of 1:9000 aerial photograph (Giuseppe and Francesco, 2013). Another way of evaluate the examined data was measured using differential leveling. This is used as a reference checkpoint. The statistical elevation value of the DSM (2010) and DSM (2016) data using these reference data gave a RMSE error value of ±0.68m and ±0.911m and Absolute mean error value of ±0.518m and ±0.897m, respectively. It has larger error relative to the other error accuracy we got from existed GCP and GPS measurements used as a reference data. And also the error value that got from the three reference were satisfies the error specification adapted by EGII. Our result sows that, the data that derived from 2010 and 2016 aerial photographs have a slight difference on the evaluate point with corresponding point of using three reference elevation points.

The distribution of the data error was tested using frequency histogram. It can be used to test whether the elevation error of the DSM data in different data collection techniques are normally distributed. It was found that, the elevation error of the DSM data derived from 2017 aerial photograph was normally distributed but, not DSM data derived from 2010 aerial photograph.

For all reference measurements, greater error value were associated with DSM data derived from 2017 aerial photograph while, smaller error associated with DSM data derived from 2010 aerial photograph, suggesting that the quality and parameter of the aerial photo taken, the height of the flight, the topographic characteristics of the study area, the distance between checkpoint taken and existed GCP point and height of the building as well as the human factor during coordinate registration can affect the DSM data.

Overall, the result obtained from our study indicated that, the accuracy of both examined data is comparable to the measured reference checkpoint from the previous studies, and the specification adopted by EGII were strongly encourage the use of both DSM data derived from aerial photograph to investigate the spatial distribution of the study area. Developments on data acquisition techniques scale and vertical spatial resolution allows the reuse and enhancement of DSM data production leading to better results for spatial investigation purpose.

CHAPTER FIVE

5. Conclusion and Recommendations

5.1. Conclusion

In this study, we evaluated the accuracy of both DSM derived from aerial photograph with existed GCP point, RTK GPS and leveling measurement as a control. We conclude that, the accuracy result of the data set yields from DSM data derived from 2010 aerial photograph was satisfied the previous finding of RMSE value of ±0.55mand the specification adopted by EGII. According to the result we got, it possible to investigate the terrain distribution involving with a grid of three times the error we got from the result. The elevation error of existed GCP we got was directly influences the error of the final product of both DSM derived from aerial photograph in the process of rectification. And also the DSM (2010) elevation data was much accurate than that of the value of DSM (2016) data set using the three reference elevation point. It is an efficient, relatively precise and accurate data for spatial modeling and investigation in the selected study area.

From the dataset we got from the result, most of DSM (2010) data set has negative value on the three reference checkpoint implies that under estimated the terrain distribution of the study area but, most of DSM (2016) data set has positive value on the three reference checkpoint elevation which upper estimated the terrain distribution of the study area. These result indicated that the vertical accuracy of both DSM elevation data was affected by the scale of aerial photograph and the use of base station as a reference data.

Overall, the result obtained from our study indicated that, the accuracy of both examined data is comparable to the measured reference checkpoint, GPS measurement technique was more appropriate for a reference to evaluate DSM data. By increasing the quality of data acquisition techniques, scale and vertical spatial resolution allows the reuse and enhancement of DSM data production leading to better results for spatial investigation purpose. Finally we conclude that, the examined data was applicable for cadastral application, road investigation, spatial modeling and risk management analysis in the study area.

5.2 Recommendations

The accuracy of DSM derived from aerial photograph can be checked by increasing the number of checkpoints. Also, recommended that the vertical accuracy assessments of DSM were analyzed by selecting the appropriate method of independent data collection techniques.

In the list of finding and conclusions reached the following recommendations are forwarded:

- Depending on the finding of observations results, the accuracy of DSM derived from aerial photograph can be checked by increasing the number of checkpoints.
- The vertical accuracy assessment of DSM was analyzed by selecting the appropriate method of independent data collection techniques.
- The value of DSM accuracy increase by increasing the scale and resolution of the aerial photograph.
- The vertical accuracy obtained from both use DSM has indicated that they can be used to develop a topographic map with a counter interval of not less than the value of three times of the value of error we got.
- The infrastructure of the existing GCP point found in the study area should be measured and/or reread again for terrain investigation purpose.

References

Arctur, D., Zeiler, M. (2004). *Designing Geodatabases*: case studies in GIS data modeling. Esri Press.

ASPRS, (2004). *ASPRS Guidelines, Vertical Accuracy Reporting for LiDAR Data*, American Society for Photogrammetry and Remote Sensing (ASPRS), Bethesda, Maryland, USA. 20 pages.

Baltsavias, E.P., (1999), A comparison between photogrammetry and laser scanning. *ISPRS Journal of Photogrammetry & Remote Sensing*, 54, 83-94.

Bolstad, P., (2005).*GIS Fundamentals (2nd Edn)*. White Bear Lake, Minnesota: Eider Press.

Burrough, A.P., and McDonnell, A.R., (1998). *Principles of geographic information systems*. Oxford University Press.

Congalton. R. G., and Green. K., (2009). *Assessing the Accuracy of Remotely Sensed Data*. Taylor and Francis. Boca Raton, London, New York.

Conolly, J., Lake, M. (2006). *Geographical Information Systems in Archaeology*. Cambridge Manuals in Archaeology. Cambridge University Press, United Kingdom

De Smith, M., Goodchild, P. Longley R., (2007). *Geospatial Analysis: A comprehensive guide to principles, techniques, and software tools*. London: Troubador.

Elangovan, K., (2006). *GIS: Fundamentals, application and implementation*, New India Publishing Agency, Jai Bharat Printing Press.

FGDC, (2008). *Geographic Information Framework Data Content Standard, Part 4: Geodetic Control*, Federal Geographic Data Committee (FGDC), Reston, Virginia. 23 pages.

Fabris M., Pesci A., (2005) - *Automated DEM extraction in digital aerial photogrammetry: Precisions and validation for mass movement monitoring.* Annals of Geophysics, 48 (6):973-988. doi: http://dx.doi.org/10.4401/ag-3247.

Gilvear, D., and Bryant, R. (2003). Analysis of aerial photography and other remotely sensed data. *Tools in Fluvial Geomorphology*. p. 135-170.

Giuseppe P., and Francesco F., (2013) DEM extraction from archive aerial photo: accuracy assessment in area of complex topography, *European Journal of remote sensing*, 46:1,363-378

Gizachew, B., (2012). *GIS for Cadastre Application*. Ethiopian Civil Service University. Addis Ababa. vol, 1. No, 2. Pp, 15-16

Greenwalt, R., and Schultz, E., (1962, 1968). *Principles of Error Theory and Cartographic Applicatio*n, Aeronautical Chart and Information Center, St, Louis, Missouri. 631118

Hodgson, M. E. and Bresnahan, P., (2004). Accuracy of airborne lidar-derived elevation: empirical assessment and error budget. *Photogrammetric Engineering and Remote Sensing*, **70**(3):335-338.

Hirt**, C., (**2015), *Digital Terrain Models*. In: Encyclopedia of Geodesy (Ed. E.W. Grafarend),doi 10.1007/978-3-319-02370-0_31-1, Springer, Berlin, Heidelberg.

ICSM. (2008). *ICSM Guidelines for Digital Elevation Data*, Inter-Governmental Committee on Surveying and Mapping (ICSM), Canberra, Australia. 49 pages.

Jarvis A., Rubiano J., Nelson A., Farrow A., Mulligan M., (2004) - *Practical use of SRTM data in the tropics: Comparisons with digital elevation models generated from Cartographic data*. Working Document: Centro International de Agricultural Tropical (CIAT), 198: 32 p.

Jensen J.R., 2007. Remote Sensing of the Environment, 2nd ed., Pearson, New York. General Survey Instruction Rules, 2015, Land Title and Survey Authority of British Columbia.

Kääb, A.; Girod, L.; Berthling, I 2014, *Surface kinematics of periglacial sorted circles using structure-from-motion technology*. Cryosphere. 8, 1041–1056.

Keplan, D. and Hegarty, J., (2006). *Understanding GPS: principle and application* (2nd edition). Artech House, doi 1-58053-894-0, London, Boston.

Krieger, G. A., Moreira, et al., (2007),*TanDEM-X: a satellite formation for high resolution SAR interferometry*. IEEETrans. Geosci. Remote Sens., 45, 3317–3341.

Leila, F, Cláudia, A., Lívia, T., Paulo G., Albuquerque, C., Oliveira F., (2012). Elevation accuracy assessment of a DSM and DTM generated for an urban area from the ALTM 2025 air bourn laser scanning sensor. *Brazilian Institute for space research*, Brazil.

Li Z, Zhu C, Gold C., (2005). *Digital terrain modeling*: principles and methodology. Boca Raton, FL: CRC Press.

Liu, X., Zhang, Z., Peterson, J. and Chandra, S., (2007). LiDAR-derived high quality ground control information and DEM for image orthorectification. *GeoInformatica*, **11**(1):37-53.

Longley, P.A., Goodchild, M.F., Maguire, D., Rhind, D.W (1999),*GeographicalInformation Systems*, Vol. 2. New York: John Wiley and Sons.

Maune, D. F., Maitra, J. B. and McKay, E. J., (2007). Accuracy Standards & Guidelines, in Maune, D. F. (Eds.), *Digital Elevation Model Technologies and Applications: The DEM Users Manual, 2nd Edition*. American Society for Photogrammetry and Remote Sensing, Bethesda, Maryland. 65-97.

Michael, G.,Linas, B., Andrius, B., (2016). *Remote sensing and GIS for cadastral surveying*. Center for cartography at the faculty of natural science, Vilnius University. no. 41, pp, 143-184.

Milliman, T., O'Keefe, J., Richardson, A.D. (2012). Digital repeat photography for phonological research in forest ecosystems. *Agric. For.Meteorol*. 152. p. 159–177.

NDEP. (2004). Guidelines for digital elevation data, Version 1.0,Feb 2018.pdf, National Digital Elevation Program (NDEP).

Qiming, Z.,2017. *Digital elevation model and digital surface model.* Hong Kong Baptist University, Hong Kong, 18 pages available from: https;//www.Researchgate.net/publication/315383809.

Rabus, B., Eineder, M., Roth, A., and Bamler, R 2003, The Shuttle Radar Topography Mission – A New Class of Digital Elevation Models Acquired by Space borne Radar. *ISPRS Journal of Photogrammetry & Remote Sensing*, 57, 241-262.

Rosnell, T.; Honkavaara, E., (2012), *Point Cloud Generation from Aerial Image Data Acquired by a Quadrocopter Type Micro Unmanned Aerial Vehicle and a Digital Still Camera*. Remote sens.v12, 453–480.

Schumann G., Matgen P., Cutler M.E.J., Black A., Hoffmann L., Pfister L. (2008) -Comparison of Remotely Sensed Water Stages from Li-DAR, Topographic Contours and SRTM. *Journal of Photogrammetry and Remote Sensing*, 63: 283-296.

Shahbazi, M.; Sohn, G.; Théau, J.; Menard, P 2015, *Development and Evaluation of a UAV-Photogrammetry System for Precise 3D Environmental Modeling*. Sensors 2015, 15, 27493–27524.

Sonnentag, O., Hufkens, K., Teshera-Sterne, C., Young, A.M., Friedl, M., Braswell,Scmandt, M. (2012). *GIS Commons*: an introductory textbook on geographic information systems.

Tahar, K.; Ahmad, A.; Akib, W.; Mohd, W. 2012,*Assessment on Ground Control Points in Unmanned Aerial System Image Processing for Slope Mapping Studies*. Int. J. Sci. Eng. v 3, 1–10.

Tahar, K.N., (2013), *An evaluation on different number of ground control points in unmanned aerial vehicle photogrammetric block*. In Proceedings of the ISPRS, International Archives of the Photogrammetry, Remote Sensing and Spatial Information Sciences, Istanbul, Turkey, 27–29. Volume XL-2/W2.

Tonkin, T.N.; Midgley, N.G 2016, Ground-Control Networks for Image Based Surface Reconstruction: *An Investigation of Optimum Survey Designs Using UAV Derived Imagery and Structure-from-Motion Photogrammetry*. Remote Sensing. **V** 8, 1–8.

Turton, D. A., (2006). *Factors Influencing ALS Accuracy*, AAMHatch Pty Ltd, Brisbane, Australia. 4 pages.

Wade, T., and Sommer, S (Ed.) (2006). *A To Z: An Illustrated Dictionary of Geographic Information Systems*. Redlands, California: ESRI Press.

Webster, T. L., (2005). LIDAR validation using GIS: a case study comparison between two LIDAR collection methods. *Geocarto International*, **20**(4):11-19.

Webster, T. L. and Dias, G., (2006). An automated GIS procedure for comparing GPS and proximal LiDAR elevations. *Computers & Geosciences*, **32**(6):713-726

Wehr, A. and Lohr, U., (1999). Airborne laser scanning - an introduction and overview. *ISPRS Journal of Photogrammetry and Remote Sensing*, **54**(2-3):68-82.

Weitkamp, C., (2005). LiDAR: introduction, in Fujii, T. and Fukuchi, T. (Eds.), *Laser Remote Sensing*. Taylor & Francis, Boca Raton, London, New York and Singapore. 1-36.